4-1-2022

Search for Gravitational Waves Associated with Gamma-Ray Bursts Detected by Fermi and Swift during the LIGO–Virgo Run O3b

LIGO Scientific Collaboration

Virgo Collaboration

KAGRA Collaboration

Tiffany Z. Summerscales
Andrews University, tzs@andrews.edu

The Astrophysical Journal, 928:186 (20pp), 2022 April 1 https://doi.org/10.3847/1538-4357/ac532b

Search for Gravitational Waves Associated with Gamma-Ray Bursts Detected by Fermi and Swift during the LIGO–Virgo Run O3b

R. Abbott[1], T. D. Abbott[2], F. Acernese[3,4], K. Ackley[5], C. Adams[6], N. Adhikari[7], R. X. Adhikari[1], V. B. Adya[8], C. Affeldt[9,10], D. Agarwal[11], M. Agathos[12,13], K. Agatsuma[14], N. Aggarwal[15], O. D. Aguiar[16], L. Aiello[17], A. Ain[18], P. Ajith[19], T. Akutsu[20,21], S. Albanesi[22], A. Allocca[4,23], P. A. Altin[8], A. Amato[24], C. Anand[5], S. Anand[1], A. Ananyeva[1], S. B. Anderson[1], W. G. Anderson[7], M. Ando[25,26], T. Andrade[27], N. Andres[28], T. Andrić[29], S. V. Angelova[30], S. Ansoldi[31,32], J. M. Antelis[33], S. Antier[34], S. Appert[1], Koji Arai[1], Koya Arai[35], Y. Arai[35], S. Araki[36], A. Araya[37], M. C. Araya[1], J. S. Areeda[38], M. Arène[34], N. Aritomi[25], N. Arnaud[39,40], S. M. Aronson[2], K. G. Arun[41], H. Asada[42], Y. Asali[43], G. Ashton[5], Y. Aso[44,45], M. Assiduo[46,47], S. M. Aston[6], P. Astone[48], F. Aubin[28], C. Austin[2], S. Babak[34], F. Badaracco[49], M. K. M. Bader[50], C. Badger[51], S. Bae[52], Y. Bae[53], A. M. Baer[54], S. Bagnasco[22], Y. Bai[1], L. Baiotti[55], J. Baird[34], R. Bajpai[56], M. Ball[57], G. Ballardin[40], S. W. Ballmer[58], A. Balsamo[54], G. Baltus[59], S. Banagiri[60], D. Bankar[11], J. C. Barayoga[1], C. Barbieri[61,62,63], B. C. Barish[1], D. Barker[64], P. Barneo[27], F. Barone[4,65], B. Barr[66], L. Barsotti[67], M. Barsuglia[34], D. Barta[68], J. Bartlett[64], M. A. Barton[20,66], I. Bartos[69], R. Bassiri[70], A. Basti[18,71], M. Bawaj[72,73], J. C. Bayley[66], A. C. Baylor[7], M. Bazzan[74,75], B. Bécsy[76], V. M. Bedakihale[77], M. Bejger[78], I. Belahcene[39], V. Benedetto[79], D. Beniwal[80], T. F. Bennett[81], J. D. Bentley[14], M. BenYaala[30], F. Bergamin[9,10], B. K. Berger[70], S. Bernuzzi[13], C. P. L. Berry[15,66], D. Bersanetti[82], A. Bertolini[50], J. Betzwieser[6], D. Beveridge[83], R. Bhandare[84], U. Bhardwaj[50,85], D. Bhattacharjee[86], S. Bhaumik[69], I. A. Bilenko[87], G. Billingsley[1], S. Bini[88,89], R. Birney[90], O. Birnholtz[91], S. Biscans[1,67], M. Bischi[46,47], S. Biscoveanu[67], A. Bisht[9,10], B. Biswas[11], M. Bitossi[18,40], M.-A. Bizouard[92], J. K. Blackburn[1], C. D. Blair[6,83], D. G. Blair[83], R. M. Blair[64], F. Bobba[93,94], N. Bode[9,10], M. Boer[92], G. Bogaert[92], M. Boldrini[48,95], L. D. Bonavena[74], F. Bondu[96], E. Bonilla[70], R. Bonnand[28], P. Booker[9,10], B. A. Boom[50], R. Bork[1], V. Boschi[18], N. Bose[97], S. Bose[11], V. Bossilkov[83], V. Boudart[59], Y. Bouffanais[74,75], A. Bozzi[40], C. Bradaschia[18], P. R. Brady[7], A. Bramley[6], A. Branch[6], M. Branchesi[29,98], J. E. Brau[57], M. Breschi[13], T. Briant[99], J. H. Briggs[66], A. Brillet[92], M. Brinkmann[9,10], P. Brockill[7], A. F. Brooks[1], J. Brooks[40], D. D. Brown[80], S. Brunett[1], G. Bruno[49], R. Bruntz[54], J. Bryant[14], T. Bulik[100], H. J. Bulten[50], A. Buonanno[101,102], R. Buscicchio[14], D. Buskulic[28], C. Buy[103], R. L. Byer[70], L. Cadonati[104], G. Cagnoli[24], C. Cahillane[64], J. Calderón Bustillo[105,106], J. D. Callaghan[66], T. A. Callister[107,108], E. Calloni[4,23], J. Cameron[83], J. B. Camp[109], M. Canepa[82,110], S. Canevarolo[111], M. Cannavacciuolo[93], K. C. Cannon[26], H. Cao[80], Z. Cao[112], E. Capocasa[20], E. Capote[58], G. Carapella[93,94], F. Carbognani[40], J. B. Carlin[113], M. F. Carney[15], M. Carpinelli[40,114,115], G. Carrillo[57], G. Carullo[18,71], T. L. Carver[17], J. Casanueva Diaz[40], C. Casentini[116,117], G. Castaldi[118], S. Caudill[50,111], M. Cavaglià[86], F. Cavalier[39], R. Cavalieri[40], M. Ceasar[119], G. Cella[18], P. Cerdá-Durán[120], E. Cesarini[117], W. Chaibi[92], K. Chakravarti[11], S. Chalathadka Subrahmanya[121], E. Champion[122], C.-H. Chan[123], C. Chan[26], C. L. Chan[106], K. Chan[106], M. Chan[124], K. Chandra[97], P. Chanial[40], S. Chao[123], P. Charlton[125], E. A. Chase[15], E. Chassande-Mottin[34], C. Chatterjee[83], Debarati Chatterjee[11], Deep Chatterjee[7], M. Chaturvedi[84], S. Chaty[34], K. Chatziioannou[1], C. Chen[126,127], H. Y. Chen[67], J. Chen[123], K. Chen[128], X. Chen[83], Y.-B. Chen[129], Y.-R. Chen[130], Z. Chen[17], H. Cheng[69], C. K. Cheong[106], H. Y. Cheung[106], H. Y. Chia[69], F. Chiadini[94,131], C-Y. Chiang[132], G. Chiarini[75], R. Chierici[133], A. Chincarini[82], M. L. Chiofalo[18,71], A. Chiummo[40], G. Cho[134], H. S. Cho[135], R. K. Choudhary[83], S. Choudhary[11], N. Christensen[92], H. Chu[128], Q. Chu[83], Y-K. Chu[132], S. Chua[8], K. W. Chung[51], G. Ciani[74,75], P. Ciecielag[78], M. Cieślar[78], M. Cifaldi[116,117], A. A. Ciobanu[80], R. Ciolfi[75,136], F. Cipriano[92], A. Cirone[82,110], F. Clara[64], E. N. Clark[137], J. A. Clark[1,104], L. Clarke[138], P. Clearwater[139], S. Clesse[140], F. Cleva[92], E. Coccia[29,98], E. Codazzo[29], P.-F. Cohadon[99], D. E. Cohen[39], L. Cohen[2], M. Colleoni[141], C. G. Collette[142], A. Colombo[61], M. Colpi[61,62], C. M. Compton[64], M. Constancio, Jr.[16], L. Conti[75], S. J. Cooper[14], P. Corban[6], T. R. Corbitt[2], I. Cordero-Carrión[143], S. Corezzi[72,73], K. R. Corley[43], N. Cornish[76], D. Corre[39], A. Corsi[144], S. Cortese[40], C. A. Costa[16], R. Cotesta[102], M. W. Coughlin[60], J.-P. Coulon[92], S. T. Countryman[43], B. Cousins[145], P. Couvares[1], D. M. Coward[83], M. J. Cowart[6], D. C. Coyne[1], R. Coyne[146], J. D. E. Creighton[7], T. D. Creighton[147], A. W. Criswell[60], M. Croquette[99], S. G. Crowder[148], J. R. Cudell[59], T. J. Cullen[2], A. Cumming[66], R. Cummings[66], L. Cunningham[66], E. Cuoco[18,40,149], M. Curyło[100], P. Dabadie[24], T. Dal Canton[39], S. Dall'Osso[29], G. Dálya[150], A. Dana[70], L. M. DaneshgaranBajastani[81], B. D'Angelo[82,110], S. Danilishin[50,151], S. D'Antonio[117], K. Danzmann[9,10], C. Darsow-Fromm[121], A. Dasgupta[77], L. E. H. Datrier[66], S. Datta[11], V. Dattilo[40], I. Dave[84], M. Davier[39], G. S. Davies[152], D. Davis[1], M. C. Davis[119], E. J. Daw[153], R. Dean[119], D. DeBra[70], M. Deenadayalan[11], J. Degallaix[154], M. De Laurentis[4,23], S. Deléglise[99], V. Del Favero[122], F. De Lillo[49], N. De Lillo[66], W. Del Pozzo[18,71], L. M. DeMarchi[15], F. De Matteis[116,117], V. D'Emilio[17], N. Demos[67], T. Dent[105], A. Depasse[49], R. De Pietri[155,156], R. De Rosa[4,23], C. De Rossi[40], R. DeSalvo[118], R. De Simone[131], S. Dhurandhar[11], M. C. Díaz[147], M. Diaz-Ortiz, Jr.[69], N. A. Didio[58], T. Dietrich[50,102], L. Di Fiore[4], C. Di Fronzo[14], C. Di Giorgio[93,94], F. Di Giovanni[120], M. Di Giovanni[29], T. Di Girolamo[4,23], A. Di Lieto[18,71], B. Ding[142], S. Di Pace[48,95], I. Di Palma[48,95], F. Di Renzo[18,71], A. K. Divakarla[69], A. Dmitriev[14], Z. Doctor[57], L. D'Onofrio[4,23], F. Donovan[67], K. L. Dooley[17], S. Doravari[11], I. Dorrington[17], M. Drago[48,95], J. C. Driggers[64], Y. Drori[1], J.-G. Ducoin[39], P. Dupej[66], O. Durante[93,94], D. D'Urso[114,115], P.-A. Duverne[39], S. E. Dwyer[64], C. Eassa[64], P. J. Easter[5], M. Ebersold[157], T. Eckhardt[121], G. Eddolls[66], B. Edelman[57], T. B. Edo[1], O. Edy[152], A. Effler[6], S. Eguchi[124], J. Eichholz[8], S. S. Eikenberry[69], M. Eisenmann[28], R. A. Eisenstein[67], A. Ejlli[17], E. Engelby[38], Y. Enomoto[25], L. Errico[4,23], R. C. Essick[158], H. Estellés[141], D. Estevez[159], Z. Etienne[160], T. Etzel[1],

M. Evans[67], T. M. Evans[6], B. E. Ewing[145], V. Fafone[29,116,117], H. Fair[58], S. Fairhurst[17], A. M. Farah[158], S. Farinon[82], B. Farr[57], W. M. Farr[107,108], N. W. Farrow[5], E. J. Fauchon-Jones[17], G. Favaro[74], M. Favata[161], M. Fays[59], M. Fazio[162], J. Feicht[1], M. M. Fejer[70], E. Fenyvesi[68,163], D. L. Ferguson[164], A. Fernandez-Galiana[67], I. Ferrante[18,71], T. A. Ferreira[16], F. Fidecaro[18,71], P. Figura[100], I. Fiori[40], M. Fishbach[15], R. P. Fisher[54], R. Fittipaldi[94,165], V. Fiumara[94,166], R. Flaminio[20,28], E. Floden[60], H. Fong[26], J. A. Font[120,167], B. Fornal[168], P. W. F. Forsyth[8], A. Franke[121], S. Frasca[48,95], F. Frasconi[18], C. Frederick[169], J. P. Freed[33], Z. Frei[150], A. Freise[170], R. Frey[57], P. Fritschel[67], V. V. Frolov[6], G. G. Fronzé[22], Y. Fujii[171], Y. Fujikawa[172], M. Fukunaga[35], M. Fukushima[21], P. Fulda[69], M. Fyffe[6], H. A. Gabbard[66], B. U. Gadre[102], J. R. Gair[102], J. Gais[106], S. Galaudage[5], R. Gamba[13], D. Ganapathy[67], A. Ganguly[19], D. Gao[173], S. G. Gaonkar[11], B. Garaventa[82,110], C. García-Núñez[90], C. García-Quirós[141], F. Garufi[4,23], B. Gateley[64], S. Gaudio[33], V. Gayathri[69], G.-G. Ge[173], G. Gemme[82], A. Gennai[18], J. George[84], O. Gerberding[121], L. Gergely[174], P. Gewecke[121], S. Ghonge[104], Abhirup Ghosh[102], Archisman Ghosh[175], Shaon Ghosh[7,161], Shrobana Ghosh[17], B. Giacomazzo[61,62,63], L. Giacoppo[48,95], J. A. Giaime[2,6], K. D. Giardina[6], D. R. Gibson[90], C. Gier[30], M. Giesler[176], P. Giri[18,71], F. Gissi[79], J. Glanzer[2], A. E. Gleckl[38], P. Godwin[145], E. Goetz[177], R. Goetz[69], N. Gohlke[9,10], B. Goncharov[5,29], G. González[2], A. Gopakumar[178], M. Gosselin[40], R. Gouaty[28], D. W. Gould[8], B. Grace[8], A. Grado[4,179], M. Granata[154], V. Granata[93], A. Grant[66], S. Gras[67], P. Grassia[1], C. Gray[64], R. Gray[66], G. Greco[72], A. C. Green[69], R. Green[17], A. M. Gretarsson[33], E. M. Gretarsson[33], D. Griffith[1], W. Griffiths[17], H. L. Griggs[104], G. Grignani[72,73], A. Grimaldi[88,89], S. J. Grimm[29,98], H. Grote[17], S. Grunewald[102], P. Gruning[39], D. Guerra[120], G. M. Guidi[46,47], A. R. Guimaraes[2], G. Guixé[27], H. K. Gulati[77], H.-K. Guo[168], Y. Guo[50], Anchal Gupta[1], Anuradha Gupta[180], P. Gupta[50,111], E. K. Gustafson[1], R. Gustafson[181], F. Guzman[182], S. Ha[183], L. Haegel[34], A. Hagiwara[35,184], S. Haino[132], O. Halim[32,185], E. D. Hall[67], E. Z. Hamilton[157], G. Hammond[66], W.-B. Han[186], M. Haney[157], J. Hanks[64], C. Hanna[145], M. D. Hannam[17], O. Hannuksela[50,111], H. Hansen[64], T. J. Hansen[33], J. Hanson[6], T. Harder[92], T. Hardwick[2], K. Haris[50,111], J. Harms[29,98], G. M. Harry[187], I. W. Harry[152], D. Hartwig[121], K. Hasegawa[35], B. Haskell[78], R. K. Hasskew[6], C.-J. Haster[67], K. Hattori[188], K. Haughian[66], H. Hayakawa[189], K. Hayama[124], F. J. Hayes[66], J. Healy[122], A. Heidmann[99], A. Heidt[9,10], M. C. Heintze[6], J. Heinze[9,10], J. Heinzel[190], H. Heitmann[92], F. Hellman[191], P. Hello[39], A. F. Helmling-Cornell[57], G. Hemming[40], M. Hendry[66], I. S. Heng[66], E. Hennes[50], J. Hennig[192], M. H. Hennig[192], A. G. Hernandez[81], F. Hernandez Vivanco[5], M. Heurs[9,10], S. Higginbotham[17], S. Hild[50,151], P. Hill[30], Y. Himemoto[193], A. S. Hines[182], Y. Hiranuma[194], N. Hirata[20], E. Hirose[35], S. Hochheim[9,10], D. Hofman[154], J. N. Hohmann[121], D. G. Holcomb[119], N. A. Holland[8], I. J. Hollows[153], Z. J. Holmes[80], K. Holt[6], D. E. Holz[158], Z. Hong[195], P. Hopkins[17], J. Hough[66], S. Hourihane[129], E. J. Howell[83], C. G. Hoy[17], D. Hoyland[14], A. Hreibi[9,10], B-H. Hsieh[35], Y. Hsu[123], G-Z. Huang[195], H-Y. Huang[132], P. Huang[173], Y-C. Huang[130], Y.-J. Huang[132], Y. Huang[67], M. T. Hübner[5], A. D. Huddart[138], B. Hughey[33], D. C. Y. Hui[196], V. Hui[28], S. Husa[141], S. H. Huttner[66], R. Huxford[145], T. Huynh-Dinh[6], S. Ide[197], B. Idzkowski[100], A. Iess[116,117], B. Ikenoue[21], S. Imam[195], K. Inayoshi[198], C. Ingram[80], Y. Inoue[128], K. Ioka[199], M. Isi[67], K. Isleif[121], K. Ito[200], Y. Itoh[201,202], B. R. Iyer[19], K. Izumi[203], V. JaberianHamedan[83], T. Jacqmin[99], S. J. Jadhav[204], S. P. Jadhav[11], A. L. James[17], A. Z. Jan[122], K. Jani[205], J. Janquart[50,111], K. Janssens[92,206], N. N. Janthalur[204], P. Jaranowski[207], D. Jariwala[69], R. Jaume[141], A. C. Jenkins[51], K. Jenner[80], C. Jeon[208], M. Jeunon[60], W. Jia[67], H.-B. Jin[209,210], G. R. Johns[54], A. W. Jones[83], D. I. Jones[211], J. D. Jones[64], P. Jones[14], R. Jones[66], R. J. G. Jonker[50], L. Ju[83], P. Jung[53], K. Jung[183], J. Junker[9,10], V. Juste[159], K. Kaihotsu[200], T. Kajita[212], M. Kakizaki[188], C. V. Kalaghatgi[17,111], V. Kalogera[15], B. Kamai[1], M. Kamiizumi[189], N. Kanda[201,202], S. Kandhasamy[11], G. Kang[213], J. B. Kanner[1], Y. Kao[123], S. J. Kapadia[19], D. P. Kapasi[8], S. Karat[1], C. Karathanasis[214], S. Karki[86], R. Kashyap[145], M. Kasprzack[1], W. Kastaun[9,10], S. Katsanevas[40], E. Katsavounidis[67], W. Katzman[6], T. Kaur[83], K. Kawabe[64], K. Kawaguchi[35], N. Kawai[215], T. Kawasaki[25], F. Kéfélian[92], D. Keitel[141], J. S. Key[216], S. Khadka[70], F. Y. Khalili[87], S. Khan[17], E. A. Khazanov[217], N. Khetan[29,98], M. Khursheed[84], N. Kijbunchoo[8], C. Kim[218], J. C. Kim[219], J. Kim[220], K. Kim[221], W. S. Kim[222], Y.-M. Kim[223], C. Kimball[15], N. Kimura[184], M. Kinley-Hanlon[66], R. Kirchhoff[9,10], J. S. Kissel[64], N. Kita[25], H. Kitazawa[200], L. Kleybolte[121], S. Klimenko[69], A. M. Knee[177], T. D. Knowles[160], E. Knyazev[67], P. Koch[9,10], G. Koekoek[50,151], Y. Kojima[224], K. Kokeyama[225], S. Koley[29], P. Kolitsidou[17], M. Kolstein[214], K. Komori[25,67], V. Kondrashov[1], A. K. H. Kong[226], A. Kontos[227], N. Koper[9,10], M. Korobko[121], K. Kotake[124], M. Kovalam[83], D. B. Kozak[1], C. Kozakai[44], R. Kozu[189], V. Kringel[9,10], N. V. Krishnendu[9,10], A. Królak[228,229], G. Kuehn[9,10], F. Kuei[123], P. Kuijer[50], A. Kumar[204], P. Kumar[176], Rahul Kumar[64], Rakesh Kumar[77], J. Kume[26], K. Kuns[67], C. Kuo[128], H-S. Kuo[195], Y. Kuromiya[200], S. Kuroyanagi[230,231], K. Kusayanagi[215], S. Kuwahara[26], K. Kwak[183], P. Lagabbe[28], D. Laghi[18,71], E. Lalande[232], T. L. Lam[106], A. Lamberts[92,233], M. Landry[64], B. B. Lane[67], R. N. Lang[67], J. Lange[164], B. Lantz[70], I. La Rosa[28], A. Lartaux-Vollard[39], P. D. Lasky[5], M. Laxen[6], A. Lazzarini[1], C. Lazzaro[74,75], P. Leaci[48,95], S. Leavey[9,10], Y. K. Lecoeuche[177], H. K. Lee[234], H. M. Lee[134], H. W. Lee[219], J. Lee[134], K. Lee[235], R. Lee[130], J. Lehmann[9,10], A. Lemaître[236], M. Leonardi[20], N. Leroy[39], N. Letendre[28], C. Levesque[232], Y. Levin[5], J. N. Leviton[181], K. Leyde[34], A. K. Y. Li[1], B. Li[123], J. Li[15], K. L. Li[237], T. G. F. Li[106], X. Li[129], C-Y. Lin[238], F-K. Lin[132], F-L. Lin[195], H. L. Lin[128], L. C.-C. Lin[183], F. Linde[50,239], S. D. Linker[81], J. N. Linley[66], T. B. Littenberg[240], G. C. Liu[126], J. Liu[9,10], K. Liu[123], X. Liu[7], F. Llamas[147], M. Llorens-Monteagudo[120], R. K. L. Lo[1], A. Lockwood[241], L. T. London[67], A. Longo[242,243], D. Lopez[157], M. Lopez Portilla[111], M. Lorenzini[116,117], V. Loriette[244], M. Lormand[6], G. Losurdo[18], T. P. Lott[104], J. D. Lough[9,10], C. O. Lousto[122], G. Lovelace[38], J. F. Lucaccioni[169], H. Lück[9,10], D. Lumaca[116,117], A. P. Lundgren[152], L.-W. Luo[132], J. E. Lynam[54], R. Macas[152], M. MacInnis[67], D. M. Macleod[17], I. A. O. MacMillan[1], A. Macquet[92], I. Magaña Hernandez[7], C. Magazzù[18], R. M. Magee[1], R. Maggiore[14], M. Magnozzi[82,110], S. Mahesh[160], E. Majorana[48,95], C. Makarem[1], I. Maksimovic[244], S. Maliakal[1], A. Malik[84], N. Man[92], V. Mandic[60], V. Mangano[48,95], J. L. Mango[245], G. L. Mansell[64,67], M. Manske[7], M. Mantovani[40], M. Mapelli[74,75],

F. Marchesoni[72,246,247], M. Marchio[20], F. Marion[28], Z. Mark[129], S. Márka[43], Z. Márka[43], C. Markakis[12], A. S. Markosyan[70], A. Markowitz[1], E. Maros[1], A. Marquina[143], S. Marsat[34], F. Martelli[46,47], I. W. Martin[66], R. M. Martin[161], M. Martinez[214], V. A. Martinez[69], V. Martinez[24], K. Martinovic[51], D. V. Martynov[14], E. J. Marx[67], H. Masalehdan[121], K. Mason[67], E. Massera[153], A. Masserot[28], T. J. Massinger[67], M. Masso-Reid[66], S. Mastrogiovanni[34], A. Matas[102], M. Mateu-Lucena[141], F. Matichard[1,67], M. Matiushechkina[9,10], N. Mavalvala[67], J. J. McCann[83], R. McCarthy[64], D. E. McClelland[8], P. K. McClincy[145], S. McCormick[6], L. McCuller[67], G. I. McGhee[66], S. C. McGuire[248], C. McIsaac[152], J. McIver[177], T. McRae[8], S. T. McWilliams[160], D. Meacher[7], M. Mehmet[9,10], A. K. Mehta[102], Q. Meijer[111], A. Melatos[113], D. A. Melchor[38], G. Mendell[64], A. Menendez-Vazquez[214], C. S. Menoni[162], R. A. Mercer[7], L. Mereni[154], K. Merfeld[57], E. L. Merilh[6], J. D. Merritt[57], M. Merzougui[92], S. Meshkov[1,297], C. Messenger[66], C. Messick[164], P. M. Meyers[113], F. Meylahn[9,10], A. Mhaske[11], A. Miani[88,89], H. Miao[14], I. Michaloliakos[69], C. Michel[154], Y. Michimura[25], H. Middleton[113], L. Milano[23], A. L. Miller[49], A. Miller[81], B. Miller[50,85], M. Millhouse[113], J. C. Mills[17], E. Milotti[32,185], O. Minazzoli[92,249], Y. Minenkov[117], N. Mio[250], Ll. M. Mir[214], M. Miravet-Tenés[120], C. Mishra[251], T. Mishra[69], T. Mistry[153], S. Mitra[11], V. P. Mitrofanov[87], G. Mitselmakher[69], R. Mittleman[67], O. Miyakawa[189], A. Miyamoto[201], Y. Miyazaki[25], K. Miyo[189], S. Miyoki[189], Geoffrey Mo[67], E. Moguel[169], K. Mogushi[86], S. R. P. Mohapatra[67], S. R. Mohite[7], I. Molina[38], M. Molina-Ruiz[191], M. Mondin[81], M. Montani[46,47], C. J. Moore[14], D. Moraru[64], F. Morawski[78], A. More[11], C. Moreno[33], G. Moreno[64], Y. Mori[200], S. Morisaki[7], Y. Moriwaki[188], B. Mours[159], C. M. Mow-Lowry[14,170], S. Mozzon[152], F. Muciaccia[48,95], Arunava Mukherjee[252], D. Mukherjee[145], Soma Mukherjee[147], Subroto Mukherjee[77], Suvodip Mukherjee[85], N. Mukund[9,10], A. Mullavey[6], J. Munch[80], E. A. Muñiz[58], P. G. Murray[66], R. Musenich[82,110], S. Muusse[80], S. L. Nadji[9,10], K. Nagano[203], S. Nagano[253], A. Nagar[22,254], K. Nakamura[20], H. Nakano[255], M. Nakano[35], R. Nakashima[215], Y. Nakayama[200], V. Napolano[40], I. Nardecchia[116,117], T. Narikawa[35], L. Naticchioni[48], B. Nayak[81], R. K. Nayak[256], R. Negishi[194], B. F. Neil[83], J. Neilson[79,94], G. Nelemans[257], T. J. N. Nelson[6], M. Nery[9,10], P. Neubauer[169], A. Neunzert[216], K. Y. Ng[67], S. W. S. Ng[80], C. Nguyen[34], P. Nguyen[57], T. Nguyen[67], L. Nguyen Quynh[258], W.-T. Ni[130,173,209], S. A. Nichols[2], A. Nishizawa[26], S. Nissanke[50,85], E. Nitoglia[133], F. Nocera[40], M. Norman[17], C. North[17], S. Nozaki[188], L. K. Nuttall[152], J. Oberling[64], B. D. O'Brien[69], Y. Obuchi[21], J. O'Dell[138], E. Oelker[66], W. Ogaki[35], G. Oganesyan[29,98], J. J. Oh[222], K. Oh[196], S. H. Oh[222], M. Ohashi[189], N. Ohishi[44], M. Ohkawa[172], F. Ohme[9,10], H. Ohta[26], M. A. Okada[16], Y. Okutani[197], K. Okutomi[189], C. Olivetto[40], K. Oohara[194], C. Ooi[25], R. Oram[6], B. O'Reilly[6], R. G. Ormiston[60], N. D. Ormsby[54], L. F. Ortega[69], R. O'Shaughnessy[122], E. O'Shea[176], S. Oshino[189], S. Ossokine[102], C. Osthelder[1], S. Otabe[215], D. J. Ottaway[80], H. Overmier[6], A. E. Pace[145], G. Pagano[18,71], M. A. Page[83], G. Pagliaroli[29,98], A. Pai[97], S. A. Pai[84], J. R. Palamos[57], O. Palashov[217], C. Palomba[48], H. Pan[123], K. Pan[130,226], P. K. Panda[204], H. Pang[128], P. T. H. Pang[50,111], C. Pankow[15], F. Pannarale[48,95], B. C. Pant[84], F. H. Panther[83], F. Paoletti[18], A. Paoli[40], A. Paolone[48,259], A. Parisi[126], H. Park[7], J. Park[260], W. Parker[6,248], D. Pascucci[50], A. Pasqualetti[40], R. Passaquieti[18,71], D. Passuello[18], M. Patel[54], M. Pathak[80], B. Patricelli[18,40], A. S. Patron[2], S. Patrone[48,95], S. Paul[57], E. Payne[5], M. Pedraza[1], M. Pegoraro[75], A. Pele[6], F. E. Peña Arellano[189], S. Penn[261], A. Perego[88,89], A. Pereira[24], T. Pereira[262], C. J. Perez[64], C. Périgois[28], C. C. Perkins[69], A. Perreca[88,89], S. Perriès[133], J. Petermann[121], D. Petterson[1], H. P. Pfeiffer[102], K. A. Pham[60], K. S. Phukon[50,239], O. J. Piccinni[48], M. Pichot[92], M. Piendibene[18,71], F. Piergiovanni[46,47], L. Pierini[48,95], V. Pierro[79,94], G. Pillant[40], M. Pillas[39], F. Pilo[18], L. Pinard[154], I. M. Pinto[79,94,263], M. Pinto[40], K. Piotrzkowski[49], M. Pirello[64], M. D. Pitkin[264], E. Placidi[48,95], L. Planas[141], W. Plastino[242,243], C. Pluchar[137], R. Poggiani[18,71], E. Polini[28], D. Y. T. Pong[106], S. Ponrathnam[11], P. Popolizio[40], E. K. Porter[34], R. Poulton[40], J. Powell[139], M. Pracchia[28], T. Pradier[159], A. K. Prajapati[77], K. Prasai[70], R. Prasanna[204], G. Pratten[14], M. Principe[79,94,263], G. A. Prodi[89,265], L. Prokhorov[14], P. Prosposito[116,117], L. Prudenzi[102], A. Puecher[50,111], M. Punturo[72], F. Puosi[18,71], P. Puppo[48], M. Pürrer[102], H. Qi[17], V. Quetschke[147], R. Quitzow-James[86], F. J. Raab[64], G. Raaijmakers[50,85], H. Radkins[64], N. Radulesco[92], P. Raffai[150], S. X. Rail[232], S. Raja[84], C. Rajan[84], K. E. Ramirez[6], T. D. Ramirez[38], A. Ramos-Buades[102], J. Rana[145], P. Rapagnani[48,95], U. D. Rapol[266], A. Ray[7], V. Raymond[17], N. Raza[177], M. Razzano[18,71], J. Read[38], L. A. Rees[187], T. Regimbau[28], L. Rei[82], S. Reid[30], S. W. Reid[54], D. H. Reitze[1,69], P. Relton[17], A. Renzini[1], P. Rettegno[22,267], M. Rezac[38], F. Ricci[48,95], D. Richards[138], J. W. Richardson[1], L. Richardson[182], G. Riemenschneider[22,267], K. Riles[181], S. Rinaldi[18,71], K. Rink[177], M. Rizzo[15], N. A. Robertson[1,66], R. Robie[1], F. Robinet[39], A. Rocchi[117], S. Rodriguez[38], L. Rolland[28], J. G. Rollins[1], M. Romanelli[96], R. Romano[3,4], C. L. Romel[64], A. Romero-Rodríguez[214], I. M. Romero-Shaw[5], J. H. Romie[6], S. Ronchini[29,98], L. Rosa[4,23], C. A. Rose[7], D. Rosińska[100], M. P. Ross[241], S. Rowan[66], S. J. Rowlinson[14], S. Roy[111], Santosh Roy[11], Soumen Roy[268], D. Rozza[114,115], P. Ruggi[40], K. Ryan[64], S. Sachdev[145], T. Sadecki[64], J. Sadiq[105], N. Sago[269], S. Saito[21], Y. Saito[189], K. Sakai[270], Y. Sakai[194], M. Sakellariadou[51], Y. Sakuno[124], O. S. Salafia[61,62,63], L. Salconi[40], M. Saleem[60], F. Salemi[88,89], A. Samajdar[50,111], E. J. Sanchez[1], J. H. Sanchez[38], L. E. Sanchez[1], N. Sanchis-Gual[271], J. R. Sanders[272], A. Sanuy[27], T. R. Saravanan[11], N. Sarin[5], B. Sassolas[154], H. Satari[83], B. S. Sathyaprakash[17,145], S. Sato[273], T. Sato[172], O. Sauter[69], R. L. Savage[64], T. Sawada[201], D. Sawant[97], H. L. Sawant[11], S. Sayah[154], D. Schaetzl[1], M. Scheel[129], J. Scheuer[15], M. Schiworski[80], P. Schmidt[14], S. Schmidt[111], R. Schnabel[121], M. Schneewind[9,10], R. M. S. Schofield[57], A. Schönbeck[121], B. W. Schulte[9,10], B. F. Schutz[9,10,17], E. Schwartz[17], J. Scott[66], S. M. Scott[8], M. Seglar-Arroyo[28], T. Sekiguchi[26], Y. Sekiguchi[274], D. Sellers[6], A. S. Sengupta[268], D. Sentenac[40], E. G. Seo[106], V. Sequino[4,23], A. Sergeev[217], Y. Setyawati[111], T. Shaffer[64], M. S. Shahriar[15], B. Shams[168], L. Shao[198], A. Sharma[29,98], P. Sharma[84], S. Sharma-Chaudhary[86], P. Shawhan[101], N. S. Shcheblanov[236], S. Shibagaki[124], M. Shikauchi[26], R. Shimizu[21], T. Shimoda[25], K. Shimode[189], H. Shinkai[275], T. Shishido[45], A. Shoda[20], D. H. Shoemaker[67], D. M. Shoemaker[164], S. ShyamSundar[84], M. Sieniawska[100], D. Sigg[64], L. P. Singer[109], D. Singh[145], N. Singh[100], A. Singha[50,151], A. M. Sintes[141], V. Sipala[114,115], V. Skliris[17], B. J. J. Slagmolen[8], T. J. Slaven-Blair[83], J. Smetana[14],

J. R. Smith[38], R. J. E. Smith[5], J. Soldateschi[47,276,277], S. N. Somala[278], K. Somiya[215], E. J. Son[222], K. Soni[11], S. Soni[2], V. Sordini[133], F. Sorrentino[82], N. Sorrentino[18,71], H. Sotani[279], R. Soulard[92], T. Souradeep[11,266], E. Sowell[144], V. Spagnuolo[50,151], A. P. Spencer[66], M. Spera[74,75], R. Srinivasan[92], A. K. Srivastava[77], V. Srivastava[58], K. Staats[15], C. Stachie[92], D. A. Steer[34], J. Steinlechner[50,151], S. Steinlechner[50,151], D. J. Stops[14], M. Stover[169], K. A. Strain[66], L. C. Strang[113], G. Stratta[47,280], A. Strunk[64], R. Sturani[262], A. L. Stuver[119], S. Sudhagar[11], V. Sudhir[67], R. Sugimoto[203,281], H. G. Suh[7], T. Z. Summerscales[282], H. Sun[83], L. Sun[8], S. Sunil[77], A. Sur[78], J. Suresh[26,35], P. J. Sutton[17], Takamasa Suzuki[172], Toshikazu Suzuki[35], B. L. Swinkels[50], M. J. Szczepańczyk[69], P. Szewczyk[100], M. Tacca[50], H. Tagoshi[35], S. C. Tait[66], H. Takahashi[283], R. Takahashi[20], A. Takamori[37], S. Takano[25], H. Takeda[25], M. Takeda[201], C. J. Talbot[30], C. Talbot[1], H. Tanaka[284], Kazuyuki Tanaka[201], Kenta Tanaka[284], Taiki Tanaka[35], Takahiro Tanaka[269], A. J. Tanasijczuk[49], S. Tanioka[20,45], D. B. Tanner[69], D. Tao[1], L. Tao[69], E. N. Tapia San Martin[20], E. N. Tapia San Martín[50], C. Taranto[116], J. D. Tasson[190], S. Telada[285], R. Tenorio[141], J. E. Terhune[119], L. Terkowski[121], M. P. Thirugnanasambandam[11], M. Thomas[6], P. Thomas[64], E. E. Thompson[104], J. E. Thompson[17], S. R. Thondapu[84], K. A. Thorne[6], E. Thrane[5], Shubhanshu Tiwari[157], Srishti Tiwari[11], V. Tiwari[17], A. M. Toivonen[60], K. Toland[66], A. E. Tolley[152], T. Tomaru[20], Y. Tomigami[201], T. Tomura[189], M. Tonelli[18,71], A. Torres-Forné[120], C. I. Torrie[1], I. Tosta e Melo[114,115], D. Töyrä[8], A. Trapananti[72,246], F. Travasso[72,246], G. Traylor[6], M. Trevor[101], M. C. Tringali[40], A. Tripathee[181], L. Troiano[94,286], A. Trovato[34], L. Trozzo[4,189], R. J. Trudeau[1], D. S. Tsai[123], D. Tsai[123], K. W. Tsang[50,111,287], T. Tsang[288], J-S. Tsao[195], M. Tse[67], R. Tso[129], K. Tsubono[25], S. Tsuchida[201], L. Tsukada[26], D. Tsuna[26], T. Tsutsui[26], T. Tsuzuki[21], K. Turbang[206,289], M. Turconi[92], D. Tuyenbayev[201], A. S. Ubhi[14], N. Uchikata[35], T. Uchiyama[189], R. P. Udall[1], A. Ueda[184], T. Uehara[290,291], K. Ueno[26], G. Ueshima[292], C. S. Unnikrishnan[178], F. Uraguchi[21], A. L. Urban[2], T. Ushiba[189], A. Utina[50,151], H. Vahlbruch[9,10], G. Vajente[1], A. Vajpeyi[5], G. Valdes[182], M. Valentini[88,89], V. Valsan[7], N. van Bakel[50], M. van Beuzekom[50], J. F. J. van den Brand[50,151,293], C. Van Den Broeck[50,111], D. C. Vander-Hyde[58], L. van der Schaaf[50], J. V. van Heijningen[49], J. Vanosky[1], M. H. P. M. van Putten[294], N. van Remortel[206], M. Vardaro[50,239], A. F. Vargas[113], V. Varma[176], M. Vasúth[68], A. Vecchio[14], G. Vedovato[75], J. Veitch[66], P. J. Veitch[80], J. Venneberg[9,10], G. Venugopalan[1], D. Verkindt[28], P. Verma[229], Y. Verma[84], D. Veske[43], F. Vetrano[46], A. Viceré[46,47], S. Vidyant[58], A. D. Viets[245], A. Vijaykumar[19], V. Villa-Ortega[105], J.-Y. Vinet[92], A. Virtuoso[32,185], S. Vitale[67], T. Vo[58], H. Vocca[72,73], E. R. G. von Reis[64], J. S. A. von Wrangel[9,10], C. Vorvick[64], S. P. Vyatchanin[87], L. E. Wade[169], M. Wade[169], K. J. Wagner[122], R. C. Walet[50], M. Walker[54], G. S. Wallace[30], L. Wallace[1], S. Walsh[7], J. Wang[173], J. Z. Wang[181], W. H. Wang[147], R. L. Ward[8], J. Warner[64], M. Was[28], T. Washimi[20], N. Y. Washington[1], J. Watchi[142], B. Weaver[64], S. A. Webster[66], M. Weinert[9,10], A. J. Weinstein[1], R. Weiss[67], C. M. Weller[241], F. Wellmann[9,10], L. Wen[83], P. Weßels[9,10], K. Wette[8], J. T. Whelan[122], D. D. White[38], B. F. Whiting[69], C. Whittle[67], D. Wilken[9,10], D. Williams[66], M. J. Williams[66], A. R. Williamson[152], J. L. Willis[1], B. Willke[9,10], D. J. Wilson[137], W. Winkler[9,10], C. C. Wipf[1], T. Wlodarczyk[102], G. Woan[66], J. Woehler[9,10], J. K. Wofford[122], I. C. F. Wong[106], C. Wu[130], D. S. Wu[9,10], H. Wu[130], S. Wu[130], D. M. Wysocki[7], L. Xiao[1], W-R. Xu[195], T. Yamada[284], H. Yamamoto[1], Kazuhiro Yamamoto[188], Kohei Yamamoto[284], T. Yamamoto[189], K. Yamashita[200], R. Yamazaki[197], F. W. Yang[168], L. Yang[162], Y. Yang[295], Yang Yang[69], Z. Yang[60], M. J. Yap[8], D. W. Yeeles[17], A. B. Yelikar[122], M. Ying[123], K. Yokogawa[200], J. Yokoyama[25,26], T. Yokozawa[189], J. Yoo[176], T. Yoshioka[200], Hang Yu[129], Haocun Yu[67], H. Yuzurihara[35], A. Zadrożny[229], M. Zanolin[33], S. Zeidler[296], T. Zelenova[40], J.-P. Zendri[75], M. Zevin[158], M. Zhan[173], H. Zhang[195], J. Zhang[83], L. Zhang[1], T. Zhang[14], Y. Zhang[182], C. Zhao[83], G. Zhao[142], Y. Zhao[20], Yue Zhao[168], Y. Zheng[86], R. Zhou[191], Z. Zhou[15], X. J. Zhu[5], Z.-H. Zhu[112], A. B. Zimmerman[164], M. E. Zucker[1,67], and J. Zweizig[1]

The LIGO Scientific Collaboration, the Virgo Collaboration, and the KAGRA Collaboration

[1] LIGO Laboratory, California Institute of Technology, Pasadena, CA 91125, USA; lsc-spokesperson@ligo.org, virgo-spokesperson@ego-gw.it, hisaaki.shinkai@oit.ac.jp
[2] Louisiana State University, Baton Rouge, LA 70803, USA
[3] Dipartimento di Farmacia, Università di Salerno, I-84084 Fisciano, Salerno, Italy
[4] INFN, Sezione di Napoli, Complesso Universitario di Monte S. Angelo, I-80126 Napoli, Italy
[5] OzGrav, School of Physics & Astronomy, Monash University, Clayton 3800, Victoria, Australia
[6] LIGO Livingston Observatory, Livingston, LA 70754, USA
[7] University of Wisconsin-Milwaukee, Milwaukee, WI 53201, USA
[8] OzGrav, Australian National University, Canberra, Australian Capital Territory 0200, Australia
[9] Max Planck Institute for Gravitational Physics (Albert Einstein Institute), D-30167 Hannover, Germany
[10] Leibniz Universität Hannover, D-30167 Hannover, Germany
[11] Inter-University Centre for Astronomy and Astrophysics, Pune 411007, India
[12] University of Cambridge, Cambridge, CB2 1TN, UK
[13] Theoretisch-Physikalisches Institut, Friedrich-Schiller-Universität Jena, D-07743 Jena, Germany
[14] University of Birmingham, Birmingham, B15 2TT, UK
[15] Center for Interdisciplinary Exploration & Research in Astrophysics (CIERA), Northwestern University, Evanston, IL 60208, USA
[16] Instituto Nacional de Pesquisas Espaciais, 12227-010 São José dos Campos, São Paulo, Brazil
[17] Gravity Exploration Institute, Cardiff University, Cardiff, CF24 3AA, UK
[18] INFN, Sezione di Pisa, I-56127 Pisa, Italy
[19] International Centre for Theoretical Sciences, Tata Institute of Fundamental Research, Bengaluru 560089, India
[20] Gravitational Wave Science Project, National Astronomical Observatory of Japan (NAOJ), Mitaka City, Tokyo 181-8588, Japan
[21] Advanced Technology Center, National Astronomical Observatory of Japan (NAOJ), Mitaka City, Tokyo 181-8588, Japan
[22] INFN Sezione di Torino, I-10125 Torino, Italy
[23] Università di Napoli "Federico II", Complesso Universitario di Monte S. Angelo, I-80126 Napoli, Italy
[24] Université de Lyon, Université Claude Bernard Lyon 1, CNRS, Institut Lumière Matière, F-69622 Villeurbanne, France
[25] Department of Physics, The University of Tokyo, Bunkyo-ku, Tokyo 113-0033, Japan

[26] Research Center for the Early Universe (RESCEU), The University of Tokyo, Bunkyo-ku, Tokyo 113-0033, Japan
[27] Institut de Ciències del Cosmos (ICCUB), Universitat de Barcelona, C/ Martí i Franquès 1, Barcelona, E-08028, Spain
[28] Laboratoire d'Annecy de Physique des Particules (LAPP), Université Grenoble Alpes, Université Savoie Mont Blanc, CNRS/IN2P3, F-74941 Annecy, France
[29] Gran Sasso Science Institute (GSSI), I-67100 L'Aquila, Italy
[30] SUPA, University of Strathclyde, Glasgow, G1 1XQ, UK
[31] Dipartimento di Scienze Matematiche, Informatiche e Fisiche, Università di Udine, I-33100 Udine, Italy
[32] INFN, Sezione di Trieste, I-34127 Trieste, Italy
[33] Embry-Riddle Aeronautical University, Prescott, AZ 86301, USA
[34] Université de Paris, CNRS, Astroparticule et Cosmologie, F-75006 Paris, France
[35] Institute for Cosmic Ray Research (ICRR), KAGRA Observatory, The University of Tokyo, Kashiwa City, Chiba 277-8582, Japan
[36] Accelerator Laboratory, High Energy Accelerator Research Organization (KEK), Tsukuba City, Ibaraki 305-0801, Japan
[37] Earthquake Research Institute, The University of Tokyo, Bunkyo-ku, Tokyo 113-0032, Japan
[38] California State University Fullerton, Fullerton, CA 92831, USA
[39] Université Paris-Saclay, CNRS/IN2P3, IJCLab, F-91405 Orsay, France
[40] European Gravitational Observatory (EGO), I-56021 Cascina, Pisa, Italy
[41] Chennai Mathematical Institute, Chennai 603103, India
[42] Department of Mathematics and Physics, Gravitational Wave Science Project, Hirosaki University, Hirosaki City, Aomori 036-8561, Japan
[43] Columbia University, New York, NY 10027, USA
[44] Kamioka Branch, National Astronomical Observatory of Japan (NAOJ), Kamioka-cho, Hida City, Gifu 506-1205, Japan
[45] The Graduate University for Advanced Studies (SOKENDAI), Mitaka City, Tokyo 181-8588, Japan
[46] Università degli Studi di Urbino "Carlo Bo", I-61029 Urbino, Italy
[47] INFN, Sezione di Firenze, I-50019 Sesto Fiorentino, Firenze, Italy
[48] INFN, Sezione di Roma, I-00185 Roma, Italy
[49] Université catholique de Louvain, B-1348 Louvain-la-Neuve, Belgium
[50] Nikhef, Science Park 105, 1098 XG Amsterdam, Netherlands
[51] King's College London, University of London, London, WC2R 2LS, UK
[52] Korea Institute of Science and Technology Information (KISTI), Yuseong-gu, Daejeon 34141, Korea
[53] National Institute for Mathematical Sciences, Yuseong-gu, Daejeon 34047, Republic of Korea
[54] Christopher Newport University, Newport News, VA 23606, USA
[55] International College, Osaka University, Toyonaka City, Osaka 560-0043, Japan
[56] School of High Energy Accelerator Science, The Graduate University for Advanced Studies (SOKENDAI), Tsukuba City, Ibaraki 305-0801, Japan
[57] University of Oregon, Eugene, OR 97403, USA
[58] Syracuse University, Syracuse, NY 13244, USA
[59] Université de Liège, B-4000 Liège, Belgium
[60] University of Minnesota, Minneapolis, MN 55455, USA
[61] Università degli Studi di Milano-Bicocca, I-20126 Milano, Italy
[62] INFN, Sezione di Milano-Bicocca, I-20126 Milano, Italy
[63] INAF, Osservatorio Astronomico di Brera sede di Merate, I-23807 Merate, Lecco, Italy
[64] LIGO Hanford Observatory, Richland, WA 99352, USA
[65] Dipartimento di Medicina, Chirurgia e Odontoiatria "Scuola Medica Salernitana", Università di Salerno, I-84081 Baronissi, Salerno, Italy
[66] SUPA, University of Glasgow, Glasgow, G12 8QQ, UK
[67] LIGO Laboratory, Massachusetts Institute of Technology, Cambridge, MA 02139, USA
[68] Wigner RCP, RMKI, H-1121 Budapest, Konkoly Thege Miklós út 29-33, Hungary
[69] University of Florida, Gainesville, FL 32611, USA
[70] Stanford University, Stanford, CA 94305, USA
[71] Università di Pisa, I-56127 Pisa, Italy
[72] INFN, Sezione di Perugia, I-06123 Perugia, Italy
[73] Università di Perugia, I-06123 Perugia, Italy
[74] Università di Padova, Dipartimento di Fisica e Astronomia, I-35131 Padova, Italy
[75] INFN, Sezione di Padova, I-35131 Padova, Italy
[76] Montana State University, Bozeman, MT 59717, USA
[77] Institute for Plasma Research, Bhat, Gandhinagar 382428, India
[78] Nicolaus Copernicus Astronomical Center, Polish Academy of Sciences, 00-716, Warsaw, Poland
[79] Dipartimento di Ingegneria, Università del Sannio, I-82100 Benevento, Italy
[80] OzGrav, University of Adelaide, Adelaide, South Australia 5005, Australia
[81] California State University, Los Angeles, 5151 State University Drive, Los Angeles, CA 90032, USA
[82] INFN, Sezione di Genova, I-16146 Genova, Italy
[83] OzGrav, University of Western Australia, Crawley, Western Australia 6009, Australia
[84] RRCAT, Indore, Madhya Pradesh 452013, India
[85] GRAPPA, Anton Pannekoek Institute for Astronomy and Institute for High-Energy Physics, University of Amsterdam, Science Park 904, 1098 XH Amsterdam, Netherlands
[86] Missouri University of Science and Technology, Rolla, MO 65409, USA
[87] Faculty of Physics, Lomonosov Moscow State University, Moscow 119991, Russia
[88] Università di Trento, Dipartimento di Fisica, I-38123 Povo, Trento, Italy
[89] INFN, Trento Institute for Fundamental Physics and Applications, I-38123 Povo, Trento, Italy
[90] SUPA, University of the West of Scotland, Paisley, PA1 2BE, UK
[91] Bar-Ilan University, Ramat Gan, 5290002, Israel
[92] Artemis, Université Côte d'Azur, Observatoire de la Côte d'Azur, CNRS, F-06304 Nice, France
[93] Dipartimento di Fisica "E.R. Caianiello", Università di Salerno, I-84084 Fisciano, Salerno, Italy
[94] INFN, Sezione di Napoli, Gruppo Collegato di Salerno, Complesso Universitario di Monte S. Angelo, I-80126 Napoli, Italy
[95] Università di Roma "La Sapienza", I-00185 Roma, Italy
[96] Univ Rennes, CNRS, Institut FOTON—UMR6082, F-3500 Rennes, France
[97] Indian Institute of Technology Bombay, Powai, Mumbai 400 076, India
[98] INFN, Laboratori Nazionali del Gran Sasso, I-67100 Assergi, Italy
[99] Laboratoire Kastler Brossel, Sorbonne Université, CNRS, ENS-Université PSL, Collège de France, F-75005 Paris, France
[100] Astronomical Observatory Warsaw University, 00-478 Warsaw, Poland

[101] University of Maryland, College Park, MD 20742, USA
[102] Max Planck Institute for Gravitational Physics (Albert Einstein Institute), D-14476 Potsdam, Germany
[103] L2IT, Laboratoire des 2 Infinis—Toulouse, Université de Toulouse, CNRS/IN2P3, UPS, F-31062 Toulouse Cedex 9, France
[104] School of Physics, Georgia Institute of Technology, Atlanta, GA 30332, USA
[105] IGFAE, Campus Sur, Universidade de Santiago de Compostela, E-15782 Spain
[106] The Chinese University of Hong Kong, Shatin, NT, Hong Kong
[107] Stony Brook University, Stony Brook, NY 11794, USA
[108] Center for Computational Astrophysics, Flatiron Institute, New York, NY 10010, USA
[109] NASA Goddard Space Flight Center, Greenbelt, MD 20771, USA
[110] Dipartimento di Fisica, Università degli Studi di Genova, I-16146 Genova, Italy
[111] Institute for Gravitational and Subatomic Physics (GRASP), Utrecht University, Princetonplein 1, 3584 CC Utrecht, Netherlands
[112] Department of Astronomy, Beijing Normal University, Beijing 100875, People's Republic of China
[113] OzGrav, University of Melbourne, Parkville, Victoria 3010, Australia
[114] Università degli Studi di Sassari, I-07100 Sassari, Italy
[115] INFN, Laboratori Nazionali del Sud, I-95125 Catania, Italy
[116] Università di Roma Tor Vergata, I-00133 Roma, Italy
[117] INFN, Sezione di Roma Tor Vergata, I-00133 Roma, Italy
[118] University of Sannio at Benevento, I-82100 Benevento, Italy and INFN, Sezione di Napoli, I-80100 Napoli, Italy
[119] Villanova University, 800 Lancaster Ave, Villanova, PA 19085, USA
[120] Departamento de Astronomía y Astrofísica, Universitat de València, E-46100 Burjassot, València, Spain
[121] Universität Hamburg, D-22761 Hamburg, Germany
[122] Rochester Institute of Technology, Rochester, NY 14623, USA
[123] National Tsing Hua University, Hsinchu City, 30013 Taiwan, Republic of China
[124] Department of Applied Physics, Fukuoka University, Jonan, Fukuoka City, Fukuoka 814-0180, Japan
[125] OzGrav, Charles Sturt University, Wagga Wagga, New South Wales 2678, Australia
[126] Department of Physics, Tamkang University, Danshui Dist., New Taipei City 25137, Taiwan
[127] Department of Physics and Institute of Astronomy, National Tsing Hua University, Hsinchu 30013, Taiwan
[128] Department of Physics, Center for High Energy and High Field Physics, National Central University, Zhongli District, Taoyuan City 32001, Taiwan
[129] CaRT, California Institute of Technology, Pasadena, CA 91125, USA
[130] Department of Physics, National Tsing Hua University, Hsinchu 30013, Taiwan
[131] Dipartimento di Ingegneria Industriale (DIIN), Università di Salerno, I-84084 Fisciano, Salerno, Italy
[132] Institute of Physics, Academia Sinica, Nankang, Taipei 11529, Taiwan
[133] Université Lyon, Université Claude Bernard Lyon 1, CNRS, IP2I Lyon / IN2P3, UMR 5822, F-69622 Villeurbanne, France
[134] Seoul National University, Seoul 08826, Republic of Korea
[135] Pusan National University, Busan 46241, Republic of Korea
[136] INAF, Osservatorio Astronomico di Padova, I-35122 Padova, Italy
[137] University of Arizona, Tucson, AZ 85721, USA
[138] Rutherford Appleton Laboratory, Didcot, OX11 0DE, UK
[139] OzGrav, Swinburne University of Technology, Hawthorn VIC 3122, Australia
[140] Université libre de Bruxelles, Avenue Franklin Roosevelt 50—1050 Bruxelles, Belgium
[141] Universitat de les Illes Balears, IAC3—IEEC, E-07122 Palma de Mallorca, Spain
[142] Université Libre de Bruxelles, Brussels B-1050, Belgium
[143] Departamento de Matemáticas, Universitat de València, E-46100 Burjassot, València, Spain
[144] Texas Tech University, Lubbock, TX 79409, USA
[145] The Pennsylvania State University, University Park, PA 16802, USA
[146] University of Rhode Island, Kingston, RI 02881, USA
[147] The University of Texas Rio Grande Valley, Brownsville, TX 78520, USA
[148] Bellevue College, Bellevue, WA 98007, USA
[149] Scuola Normale Superiore, Piazza dei Cavalieri, 7—I-56126 Pisa, Italy
[150] MTA-ELTE Astrophysics Research Group, Institute of Physics, Eötvös University, Budapest 1117, Hungary
[151] Maastricht University, P.O. Box 616, 6200 MD Maastricht, Netherlands
[152] University of Portsmouth, Portsmouth, PO1 3FX, UK
[153] The University of Sheffield, Sheffield, S10 2TN, UK
[154] Université Lyon, Université Claude Bernard Lyon 1, CNRS, Laboratoire des Matériaux Avancés (LMA), IP2I Lyon / IN2P3, UMR 5822, F-69622 Villeurbanne, France
[155] Dipartimento di Scienze Matematiche, Fisiche e Informatiche, Università di Parma, I-43124 Parma, Italy
[156] INFN, Sezione di Milano Bicocca, Gruppo Collegato di Parma, I-43124 Parma, Italy
[157] Physik-Institut, University of Zurich, Winterthurerstrasse 190, 8057 Zurich, Switzerland
[158] University of Chicago, Chicago, IL 60637, USA
[159] Université de Strasbourg, CNRS, IPHC UMR 7178, F-67000 Strasbourg, France
[160] West Virginia University, Morgantown, WV 26506, USA
[161] Montclair State University, Montclair, NJ 07043, USA
[162] Colorado State University, Fort Collins, CO 80523, USA
[163] Institute for Nuclear Research, Hungarian Academy of Sciences, Bem t'er 18/c, H-4026 Debrecen, Hungary
[164] Department of Physics, University of Texas, Austin, TX 78712, USA
[165] CNR-SPIN, c/o Università di Salerno, I-84084 Fisciano, Salerno, Italy
[166] Scuola di Ingegneria, Università della Basilicata, I-85100 Potenza, Italy
[167] Observatori Astronòmic, Universitat de València, E-46980 Paterna, València, Spain
[168] The University of Utah, Salt Lake City, UT 84112, USA
[169] Kenyon College, Gambier, OH 43022, USA
[170] Vrije Universiteit Amsterdam, 1081 HV, Amsterdam, Netherlands
[171] Department of Astronomy, The University of Tokyo, Mitaka City, Tokyo 181-8588, Japan
[172] Faculty of Engineering, Niigata University, Nishi-ku, Niigata City, Niigata 950-2181, Japan
[173] State Key Laboratory of Magnetic Resonance and Atomic and Molecular Physics, Innovation Academy for Precision Measurement Science and Technology (APM), Chinese Academy of Sciences, Xiao Hong Shan, Wuhan 430071, People's Republic of China
[174] University of Szeged, Dóm tér 9, Szeged 6720, Hungary

[175] Universiteit Gent, B-9000 Gent, Belgium
[176] Cornell University, Ithaca, NY 14850, USA
[177] University of British Columbia, Vancouver, BC V6T 1Z4, Canada
[178] Tata Institute of Fundamental Research, Mumbai 400005, India
[179] INAF, Osservatorio Astronomico di Capodimonte, I-80131 Napoli, Italy
[180] The University of Mississippi, University, MS 38677, USA
[181] University of Michigan, Ann Arbor, MI 48109, USA
[182] Texas A&M University, College Station, TX 77843, USA
[183] Department of Physics, Ulsan National Institute of Science and Technology (UNIST), Ulju-gun, Ulsan 44919, Republic of Korea
[184] Applied Research Laboratory, High Energy Accelerator Research Organization (KEK), Tsukuba City, Ibaraki 305-0801, Japan
[185] Dipartimento di Fisica, Università di Trieste, I-34127 Trieste, Italy
[186] Shanghai Astronomical Observatory, Chinese Academy of Sciences, Shanghai 200030, People's Republic of China
[187] American University, Washington, D.C. 20016, USA
[188] Faculty of Science, University of Toyama, Toyama City, Toyama 930-8555, Japan
[189] Institute for Cosmic Ray Research (ICRR), KAGRA Observatory, The University of Tokyo, Kamioka-cho, Hida City, Gifu 506-1205, Japan
[190] Carleton College, Northfield, MN 55057, USA
[191] University of California, Berkeley, CA 94720, USA
[192] Maastricht University, 6200 MD, Maastricht, Netherlands
[193] College of Industrial Technology, Nihon University, Narashino City, Chiba 275-8575, Japan
[194] Graduate School of Science and Technology, Niigata University, Nishi-ku, Niigata City, Niigata 950-2181, Japan
[195] Department of Physics, National Taiwan Normal University, Sec. 4, Taipei 116, Taiwan
[196] Astronomy & Space Science, Chungnam National University, Yuseong-gu, Daejeon 34134, Korea, Republic of Korea
[197] Department of Physics and Mathematics, Aoyama Gakuin University, Sagamihara City, Kanagawa 252-5258, Japan
[198] Kavli Institute for Astronomy and Astrophysics, Peking University, Haidian District, Beijing 100871, People's Republic of China
[199] Yukawa Institute for Theoretical Physics (YITP), Kyoto University, Sakyou-ku, Kyoto City, Kyoto 606-8502, Japan
[200] Graduate School of Science and Engineering, University of Toyama, Toyama City, Toyama 930-8555, Japan
[201] Department of Physics, Graduate School of Science, Osaka City University, Sumiyoshi-ku, Osaka City, Osaka 558-8585, Japan
[202] Nambu Yoichiro Institute of Theoretical and Experimental Physics (NITEP), Osaka City University, Sumiyoshi-ku, Osaka City, Osaka 558-8585, Japan
[203] Institute of Space and Astronautical Science (JAXA), Chuo-ku, Sagamihara City, Kanagawa 252-0222, Japan
[204] Directorate of Construction, Services & Estate Management, Mumbai 400094, India
[205] Vanderbilt University, Nashville, TN 37235, USA
[206] Universiteit Antwerpen, Prinsstraat 13, B-2000 Antwerpen, Belgium
[207] University of Białystok, 15-424 Białystok, Poland
[208] Department of Physics, Ewha Womans University, Seodaemun-gu, Seoul 03760, Republic of Korea
[209] National Astronomical Observatories, Chinese Academic of Sciences, Chaoyang District, Beijing, People's Republic of China
[210] School of Astronomy and Space Science, University of Chinese Academy of Sciences, Chaoyang District, Beijing, People's Republic of China
[211] University of Southampton, Southampton, SO17 1BJ, UK
[212] Institute for Cosmic Ray Research (ICRR), The University of Tokyo, Kashiwa City, Chiba 277-8582, Japan
[213] Chung-Ang University, Seoul 06974, Republic of Korea
[214] Institut de Física d'Altes Energies (IFAE), Barcelona Institute of Science and Technology, and ICREA, E-08193 Barcelona, Spain
[215] Graduate School of Science, Tokyo Institute of Technology, Meguro-ku, Tokyo 152-8551, Japan
[216] University of Washington Bothell, Bothell, WA 98011, USA
[217] Institute of Applied Physics, Nizhny Novgorod, 603950, Russia
[218] Ewha Womans University, Seoul 03760, Republic of Korea
[219] Inje University Gimha, South Gyeongsang 50834, Republic of Korea
[220] Department of Physics, Myongji University, Yongin 17058, Republic of Korea
[221] Korea Astronomy and Space Science Institute, Daejeon 34055, Republic of Korea
[222] National Institute for Mathematical Sciences, Daejeon 34047, Republic of Korea
[223] Ulsan National Institute of Science and Technology, Ulsan 44919, Republic of Korea
[224] Department of Physical Science, Hiroshima University, Higashihiroshima City, Hiroshima 903-0213, Japan
[225] School of Physics and Astronomy, Cardiff University, Cardiff, CF24 3AA, UK
[226] Institute of Astronomy, National Tsing Hua University, Hsinchu 30013, Taiwan
[227] Bard College, 30 Campus Rd, Annandale-On-Hudson, NY 12504, USA
[228] Institute of Mathematics, Polish Academy of Sciences, 00656 Warsaw, Poland
[229] National Center for Nuclear Research, 05-400 Świerk-Otwock, Poland
[230] Instituto de Fisica Teorica, E-28049 Madrid, Spain
[231] Department of Physics, Nagoya University, Chikusa-ku, Nagoya, Aichi 464-8602, Japan
[232] Université de Montréal/Polytechnique, Montreal, Quebec, H3T 1J4, Canada
[233] Laboratoire Lagrange, Université Côte d'Azur, Observatoire Côte d'Azur, CNRS, F-06304 Nice, France
[234] Department of Physics, Hanyang University, Seoul 04763, Republic of Korea
[235] Sungkyunkwan University, Seoul 03063, Republic of Korea
[236] NAVIER, École des Ponts, Univ Gustave Eiffel, CNRS, Marne-la-Vallée, France
[237] Department of Physics, National Cheng Kung University, Tainan City 701, Taiwan
[238] National Center for High-performance computing, National Applied Research Laboratories, Hsinchu Science Park, Hsinchu City 30076, Taiwan
[239] Institute for High-Energy Physics, University of Amsterdam, Science Park 904, 1098 XH Amsterdam, Netherlands
[240] NASA Marshall Space Flight Center, Huntsville, AL 35811, USA
[241] University of Washington, Seattle, WA 98195, USA
[242] Dipartimento di Matematica e Fisica, Università degli Studi Roma Tre, I-00146 Roma, Italy
[243] INFN, Sezione di Roma Tre, I-00146 Roma, Italy
[244] ESPCI, CNRS, F-75005 Paris, France
[245] Concordia University Wisconsin, Mequon, WI 53097, USA
[246] Università di Camerino, Dipartimento di Fisica, I-62032 Camerino, Italy
[247] School of Physics Science and Engineering, Tongji University, Shanghai 200092, China
[248] Southern University and A&M College, Baton Rouge, LA 70813, USA
[249] Centre Scientifique de Monaco, 8 quai Antoine Ier, MC-98000, Monaco
[250] Institute for Photon Science and Technology, The University of Tokyo, Bunkyo-ku, Tokyo 113-8656, Japan

[251] Indian Institute of Technology Madras, Chennai 600036, India
[252] Saha Institute of Nuclear Physics, Bidhannagar, West Bengal 700064, India
[253] The Applied Electromagnetic Research Institute, National Institute of Information and Communications Technology (NICT), Koganei City, Tokyo 184-8795, Japan
[254] Institut des Hautes Etudes Scientifiques, F-91440 Bures-sur-Yvette, France
[255] Faculty of Law, Ryukoku University, Fushimi-ku, Kyoto City, Kyoto 612-8577, Japan
[256] Indian Institute of Science Education and Research, Kolkata, Mohanpur, West Bengal 741252, India
[257] Department of Astrophysics/IMAPP, Radboud University Nijmegen, P.O. Box 9010, 6500 GL Nijmegen, Netherlands
[258] Department of Physics, University of Notre Dame, Notre Dame, IN 46556, USA
[259] Consiglio Nazionale delle Ricerche—Istituto dei Sistemi Complessi, Piazzale Aldo Moro 5, I-00185 Roma, Italy
[260] Korea Astronomy and Space Science Institute (KASI), Yuseong-gu, Daejeon 34055, Republic of Korea
[261] Hobart and William Smith Colleges, Geneva, NY 14456, USA
[262] International Institute of Physics, Universidade Federal do Rio Grande do Norte, Natal RN 59078-970, Brazil
[263] Museo Storico della Fisica e Centro Studi e Ricerche "Enrico Fermi", I-00184 Roma, Italy
[264] Lancaster University, Lancaster, LA1 4YW, UK
[265] Università di Trento, Dipartimento di Matematica, I-38123 Povo, Trento, Italy
[266] Indian Institute of Science Education and Research, Pune, Maharashtra 411008, India
[267] Dipartimento di Fisica, Università degli Studi di Torino, I-10125 Torino, Italy
[268] Indian Institute of Technology, Palaj, Gandhinagar, Gujarat 382355, India
[269] Department of Physics, Kyoto University, Sakyou-ku, Kyoto City, Kyoto 606-8502, Japan
[270] Department of Electronic Control Engineering, National Institute of Technology, Nagaoka College, Nagaoka City, Niigata 940-8532, Japan
[271] Departamento de Matemática da Universidade de Aveiro and Centre for Research and Development in Mathematics and Applications, Campus de Santiago, 3810-183 Aveiro, Portugal
[272] Marquette University, 11420 West Clybourn Street, Milwaukee, WI 53233, USA
[273] Graduate School of Science and Engineering, Hosei University, Koganei City, Tokyo 184-8584, Japan
[274] Faculty of Science, Toho University, Funabashi City, Chiba 274-8510, Japan
[275] Faculty of Information Science and Technology, Osaka Institute of Technology, Hirakata City, Osaka 573-0196, Japan
[276] Università di Firenze, Sesto Fiorentino I-50019, Italy
[277] INAF, Osservatorio Astrofisico di Arcetri, Largo Enrico Fermi 5, I-50125 Firenze, Italy
[278] Indian Institute of Technology Hyderabad, Sangareddy, Khandi, Telangana 502285, India
[279] iTHEMS (Interdisciplinary Theoretical and Mathematical Sciences Program), The Institute of Physical and Chemical Research (RIKEN), Wako, Saitama 351-0198, Japan
[280] INAF, Osservatorio di Astrofisica e Scienza dello Spazio, I-40129 Bologna, Italy
[281] Department of Space and Astronautical Science, The Graduate University for Advanced Studies (SOKENDAI), Sagamihara City, Kanagawa 252-5210, Japan
[282] Andrews University, Berrien Springs, MI 49104, USA
[283] Research Center for Space Science, Advanced Research Laboratories, Tokyo City University, Setagaya, Tokyo 158-0082, Japan
[284] Institute for Cosmic Ray Research (ICRR), Research Center for Cosmic Neutrinos (RCCN), The University of Tokyo, Kashiwa City, Chiba 277-8582, Japan
[285] National Metrology Institute of Japan, National Institute of Advanced Industrial Science and Technology, Tsukuba City, Ibaraki 305-8568, Japan
[286] Dipartimento di Scienze Aziendali—Management and Innovation Systems (DISA-MIS), Università di Salerno, I-84084 Fisciano, Salerno, Italy
[287] Van Swinderen Institute for Particle Physics and Gravity, University of Groningen, Nijenborgh 4, 9747 AG Groningen, Netherlands
[288] Faculty of Science, Department of Physics, The Chinese University of Hong Kong, Shatin, N.T., Hong Kong
[289] Vrije Universiteit Brussel, Boulevard de la Plaine 2, 1050 Ixelles, Belgium
[290] Department of Communications Engineering, National Defense Academy of Japan, Yokosuka City, Kanagawa 239-8686, Japan
[291] Department of Physics, University of Florida, Gainesville, FL 32611, USA
[292] Department of Information and Management Systems Engineering, Nagaoka University of Technology, Nagaoka City, Niigata 940-2188, Japan
[293] Vrije Universiteit Amsterdam, 1081 HV Amsterdam, Netherlands
[294] Department of Physics and Astronomy, Sejong University, Gwangjin-gu, Seoul 143-747, Repubic of Korea
[295] Department of Electrophysics, National Chiao Tung University, Hsinchu, Taiwan
[296] Department of Physics, Rikkyo University, Toshima-ku, Tokyo 171-8501, Japan
Received 2021 November 6; revised 2022 February 4; accepted 2022 February 7; published 2022 April 12

Abstract

We search for gravitational-wave signals associated with gamma-ray bursts (GRBs) detected by the Fermi and Swift satellites during the second half of the third observing run of Advanced LIGO and Advanced Virgo (2019 November 1 15:00 UTC–2020 March 27 17:00 UTC). We conduct two independent searches: a generic gravitational-wave transients search to analyze 86 GRBs and an analysis to target binary mergers with at least one neutron star as short GRB progenitors for 17 events. We find no significant evidence for gravitational-wave signals associated with any of these GRBs. A weighted binomial test of the combined results finds no evidence for subthreshold gravitational-wave signals associated with this GRB ensemble either. We use several source types and signal morphologies during the searches, resulting in lower bounds on the estimated distance to each GRB. Finally, we constrain the population of low-luminosity short GRBs using results from the first to the third observing runs of Advanced LIGO and Advanced Virgo. The resulting population is in accordance with the local binary neutron star merger rate.

[297] Deceased, August 2020.

Unified Astronomy Thesaurus concepts: Gamma-ray bursts (629); Gravitational wave astronomy (675); Gravitational waves (678); Gravitational wave detectors (676)

1. Introduction

Gamma-ray bursts (GRBs; Kumar & Zhang 2015) are intense and highly variable flashes of gamma-rays (the prompt emission), followed by a long-lasting, multiwavelength emission (the afterglow emission), typically observed in X-rays, optical, radio, and sometimes in gamma-rays. They are believed to be powered by ultra-relativistic jets produced by rapid accretion onto a central compact object: a black hole (BH; Woosley 1993; Popham et al. 1999) or a magnetar (Dai & Lu 1998; Zhang & Mészáros 2001).

GRBs are divided into two classes, depending on the duration and the spectral hardness of the prompt emission (Kouveliotou et al. 1993): long, soft GRBs (duration $\gtrsim$2 s) and short, hard GRBs (duration $<$2 s).

Long GRBs are thought to be associated with the core collapse of massive stars. This connection is observationally supported by the identification of supernova (SN) signatures in a number of sufficiently close long GRBs (Galama et al. 1998; Hjorth et al. 2003; Stanek et al. 2003). Core-collapsing massive stars are also expected to emit gravitational waves (GWs) if there is some asymmetry in the stellar-envelope ejection phase (Kotake et al. 2006; Ott 2009; Gossan et al. 2016). State-of-the-art models predict that such GW radiation can be detected by current generation GW interferometers only within our galaxy (Abbott et al. 2020); however, according to more extreme phenomenological models, such as long-lived bar-mode instabilities and disk fragmentation instabilities, GW radiation could be detected even for extragalactic sources (Fryer et al. 2002; van Putten et al. 2004; Piro & Pfahl 2007; Corsi & Mészáros 2009; Gossan et al. 2016; Abbott et al. 2020).

Short GRBs were long believed to be associated with compact binary coalescence (CBC) composed of two neutron stars (NSs), a binary neutron star (BNS) system, or an NS and a BH, an NSBH binary (Eichler et al. 1989; Paczynski 1991; Narayan et al. 1992). The definitive proof of this association (Abbott et al. 2017a, 2017d) came with the joint detection of the BNS merger GW signal GW170817 (Abbott et al. 2017c, 2019c) and GRB 170817A (Goldstein et al. 2017; Savchenko et al. 2017). The groundbreaking electromagnetic follow-up campaign performed after this joint detection allowed the identification of the associated kilonova emission and of the GRB afterglow emission (see Abbott et al. (2017d) and references therein).

GRB 170817A was 2–6 orders of magnitude less energetic than other GRBs (Abbott et al. 2017a); the low luminosity of this source, together with the delayed onset and rising multiwavelength light curve of the afterglow (Haggard et al. 2017; Hallinan et al. 2017; Troja et al. 2017; D'Avanzo et al. 2018; Lyman et al. 2018) suggested an off-axis GRB with a relativistic structured jet or a cocoon emission from the relativistic jet shocking its surrounding nonrelativistic material. Late time multiwavelength observations were crucial to discriminate between these scenarios, and now it is widely accepted that GRB 170817A originated from a structured jet observed off-axis (see, e.g., Lamb et al. 2018; Mooley et al. 2018; Troja et al. 2018, 2019; Ghirlanda et al. 2019).

In Abbott et al. (2020) we presented targeted GW follow-up of GRBs reported during the first part of the third observing run of Advanced LIGO and Advanced Virgo (O3a; 2019 April 1 15:00 UTC–2019 October 1 15:00 UTC) by Fermi's Gamma-Ray Burst Monitor (Fermi/GBM; Meegan et al. 2009) and Swift's Burst Alert Telescope (Swift/BAT; Gehrels et al. 2004; Barthelmy et al. 2005; Tohuvavohu et al. 2020). No significant evidence for GW signals associated with the GRBs that have been followed up on has been found, nor for a population of unidentified subthreshold signals.

In this paper we present targeted GW follow-up of GRBs reported during the second part of the third observing run of Advanced LIGO and Advanced Virgo (O3b) by Fermi/GBM and Swift/BAT. O3b took place between 2019 November 1 15:00 UTC and 2020 March 27 17:00 UTC. During O3b, 35 CBC events have been identified with an inferred probability of astrophysical CBC origin of $p_{\rm astro} > 0.5$ (Abbott et al. 2021a). The majority of them are classified as mergers of binary black hole (BBH) systems; however, several events are consistent with binary systems with at least one NS (Abbott et al. 2021a). One other event with lower $p_{\rm astro}$ was also published as a possible NSBH coalescence (Abbott et al. 2021b). No EM counterparts have been reported so far in association with these events; however, given their large distances ($\gtrsim$300 Mpc) and their large error in the sky localization (Abbott et al. 2021a), it would have been difficult to detect an EM signal in association with these GW events.

In Section 2 we discuss the sample of GRBs analyzed in this paper. In Section 3 we summarize the methods used to follow up on GRBs. In Section 4 we describe the results, and in Section 5 we present a population model analysis. Finally, in Section 6 we present our concluding remarks.

2. GRBs During O3b

Our GRB sample consists of 108 events that occurred between 2019 November 1 15:00 UTC and 2020 March 27 17:00 UTC. The vast majority of these events were identified in low-latency via notices circulated by the Gamma-ray Coordinates Network (GCN) and subsequently refined with additional data from the Swift/BAT catalog and the Fermi/GBM catalog.[298] The Vetting Automation and Literature Informed Database (Coyne 2015) is a dedicated processing system that tracks updates to the observed GRB parameters, comparing time and localization data to ensure that the latest results are used for our GW analyses, and employing an automated literature search to identify particularly noteworthy events.

We identify candidate events by classifying each GRB as *long*, *short*, or *ambiguous*. We classify events based on their T_{90} (and its associated error δT_{90}), which is the time interval over which 90% of the total background-subtracted photon counts are observed. GRBs are classified as *short* when $T_{90} + |\delta T_{90}| < 2$ s, GRBs are classified as *long* when $T_{90} - |\delta T_{90}| > 4$ s, and all remaining GRBs are labeled as *ambiguous*. This long/short classification based on duration is only a general trend, and is not a perfect discriminator. In particular, it does not account for short GRBs that are followed by periods

[298] Swift/BAT Gamma-Ray Burst Catalog swift.gsfc.nasa.gov/results/batgrbcat/, and Fermi/GBM Burst Catalog heasarc.gsfc.nasa.gov/W3Browse/fermi/fermigbrst.html.

of extended emission (Norris & Bonnell 2006), for which measures of T_{90} may substantially exceed these thresholds. For more robust classification one must also consider spectral properties, most commonly the spectral hardness or peak energy of the event, but since our sample consists of observations from multiple observatories with different spectral sensitivities we do not employ such quantities when organizing our sample.

This classification process results in seven short GRBs, 12 ambiguous GRBs, and 89 long GRBs. Of all these GRBs, only two have known redshifts:

1. GRB 191221B ($z = 1.148$; Kuin & Swift/UVOT Team 2019; Vielfaure et al. 2019)
2. GRB 200205B ($z = 1.465$; Vielfaure et al. 2020)

In keeping with previous studies of this kind (Abbott et al. 2017e, 2019d, 2020), we apply a generic transient search to all events, regardless of classification. In order to maximize our chances at identifying potential CBC candidates, we apply our modeled search to all short and ambiguous GRBs. We also follow the same requirements on amount of data available within our network to process a given GRB. For the modeled search we select GRBs if there is a minimum amount of time in at least one detector around the time of the event. This gives us 17 events for our analysis corresponding with the observing time for the same selection criteria (96.6% with at least one interferometer in observing mode). For the generic transient search, we perform the selection by requiring enough data in at least two interferometers. This leads to 86 GRBs to analyze and is also compatible with the network observing time of at least two detectors (85.3%).

3. Search Methods

3.1. Modeled Search for Compact Binary Mergers

This analysis is carried out by a coherent matched filtering pipeline, `PyGRB` (Harry & Fairhurst 2011; Williamson et al. 2014), contained within the open-source `PyCBC` (Nitz et al. 2020) suite, which also relies heavily on the LALSuite (LIGO Scientific Collaboration 2018) library. These searches seek to find candidate GW signals coincident with the GRB triggers due to the inspiral and merger of BNS or NSBH binaries. We define a window around each GRB trigger, the *on-source window*, which is $[-5, +1]$ s from the GRB trigger time. This window is based on the assumption that a GW may precede the prompt GRB emission by several seconds (Lee & Ramirez-Ruiz 2007; Vedrenne & Atteia 2009), and was demonstrated by GW170817 (Abbott et al. 2017b). The search also uses time surrounding the trigger, split into 6 s *off-source windows*, to estimate the background. In total, the search uses ∼90 minutes of data around each GRB trigger to assign a significance to candidate events by ranking them against the background. To constrain the sky location of the GRB event, the search is using a grid based on the best localization known either from Fermi/GBM or Swift/BAT.

The analysis requires a bank of template waveforms to carry out the matched filtering. We generated this bank using both geometric (Brown et al. 2012; Harry et al. 2014) and stochastic methods (Harry et al. 2008) for BNS and NSBH signals. The waveforms used in generating this bank are phenomenological inspiral–merger–ringdown waveform models of the IMRPhenomD family (Husa et al. 2016; Khan et al. 2016). We choose to place limits on the bank, identical to those used in the O3a template bank (Abbott et al. 2020), such that any NS masses are limited to $[1.0, 2.8]M_{\odot}$ and BH masses are within $[2.8, 25]M_{\odot}$. We conservatively set the mass cutoff between an NS and a BH based on an NS equation of state (Kalogera & Baym 1996). Functionally, this cutoff has no effect on the waveforms and is just used for nomenclature. The bank only contains aligned-spin BNS and NSBH binaries where the maximum dimensionless spin magnitude for NSs is 0.05 from the largest observed NS spin in a binary (Burgay et al. 2003). For BH, we limit the spin to 0.998 based on theory (Thorne 1974). Finally, we check to ensure that all potential binaries are viable GRB progenitors with the creation of an accretion disk able to power a GRB (Pannarale & Ohme 2014). We focus the search on these types of compact binary events as they are the most likely GRB progenitors. Certain conditions may be able to produce short-GRB-like events without the formation of an accretion disk, as in the case of theorized resonant shattering flares (RSFs) acting as a precursor GRB to an otherwise electromagnetically dark NSBH event (Tsang et al. 2012; Tsang 2013; Neill et al. 2021). Our search does not presently include these cases, as doing so would increase both the computing cost of the search and its false-alarm probability, potentially reducing the sensitivity of signals associated with accretion disk formation. This choice may be revisited in the future, especially in light of additional evidence for RSFs.

The only structural change between this bank and the bank used in the O3a modeled searches (Abbott et al. 2020) is the template placement for NSBH systems with total mass $M < 6M_{\odot}$. Both banks are constructed by first performing a geometric generation for a part of the parameter space. These templates are then seeded to a stochastic generation that fills the rest of the parameter space (Capano et al. 2016). The difference between the O3a and O3b banks is that the geometric generation for the O3a bank extended through the low-mass NSBH region whereas the O3b bank limits the geometric generation to the BNS region. We made this change based on a bank verification that tests a bank's ability to recover a set of signals. The result of this verification is a fitting factor ($\mathcal{FF}$) that quantitatively measures the bank's performance (Apostolatos 1995). The target for our template banks is to minimize the number of signals that have a $\mathcal{FF}$ less than a threshold, which we set at 0.97 for our offline searches. For the same set of signals in the low-mass NSBH region, the bank with a limited geometric generation recovers a factor of 10 less signals with a fitting factor below 0.97—when compared to the extended geometric bank. These results show that the limited geometric approach creates a more sensitive template bank for our searches.

`PyGRB` uses this bank to rank candidate signals based on a re-weighted optimal signal-to noise ratio (S/N). This optimal S/N is the result of the coherent matched filter, and is re-weighted by how well the template matches the identified signal (Harry & Fairhurst 2011; Williamson et al. 2014). The search can then rank the significance of any event against the background using the *off-source* windows. In order to improve this ranking statistic, we artificially increase the amount of off-source data by performing *time slides* (Williamson et al. 2014).

To further determine the sensitivity of our searches, we inject signals into the off-source data and attempt to recover them. The signals that we choose to inject are generally in the same BNS and NSBH domains as the template bank, with a few

important distinctions. Again, we replicate what was done in O3a (Abbott et al. 2020), where the injected signals are split into three sets; a BNS set with non-aligned (precessing) spins, an aligned-spin NSBH set, and a precessing NSBH set. The NS masses in a BNS binary are selected randomly from a normal distribution with a mean of $1.4M_{\odot}$ and variance of $0.2M_{\odot}$ (Özel et al. 2012). For NSBH binaries, NS masses are selected from a normal distribution with slightly more variance ($\mu = 1.4M_{\odot}$, $\sigma = 0.4M_{\odot}$). The larger width reflects the greater uncertainty arising from a lack of observed NSBH systems. BH masses are randomly selected from the following normal distribution ($\mu = 10.0M_{\odot}$, $\sigma = 6.0M_{\odot}$). For all cases we place limits on the distributions similar to those used for the template bank. Randomly selected spin magnitudes are less than 0.4 for NSs based on the maximum observed pulsar spin (Hessels et al. 2006), and less than 0.98 for BHs (Miller & Miller 2014). For the two sets of injections that allow precessing signals, the orientations are also randomly selected. We also choose to use different waveform families than the ones used to generate the template bank to account for modeling uncertainty. We generate the BNS injections using the SpinTaylorT2 family, which are post-Newtonian approximations in the time domain (Sathyaprakash & Dhurandhar 1991; Blanchet et al. 1996; Mikoczi et al. 2005; Arun et al. 2009; Bohé et al. 2013, 2015; Mishra et al. 2016). The NSBH sets both make use of the SEOBNRv3 family of waveforms. These waveforms are effective-one-body approximates that are tuned for precessing systems (Pan et al. 2014; Taracchini et al. 2014; Babak et al. 2017). As with the template bank, we check to ensure that generated systems are capable GRB progenitors (Pannarale & Ohme 2014). These injection sets allow us to calculate the 90% exclusion distance (D_{90}), which is the distance at which we recover 90% of the injected signals with a significant ranking statistic.

3.2. Search for Generic GW Transients

This analysis, carried out with the `X-Pipeline` software package (Sutton et al. 2010; Was et al. 2012), searches for excess power that is coherent across the GW detector network and consistent with the sky localization and time window of each GRB. Like the previous `X-Pipeline` analyses (Abbott et al. 2017e, 2019d, 2020), the search time window starts 600 s before the GRB trigger time and ends at 60 s after trigger time, or at T_{90} if $T_{90} > 60$ s. This is sufficient to cover the time delay between GW emission from a progenitor and any GRB prompt emission (Koshut et al. 1995; Aloy et al. 2000; MacFadyen et al. 2001; Zhang et al. 2003; Lazzati 2005; Wang & Mészáros 2007; Burlon et al. 2008, 2009; Lazzati et al. 2009; Vedrenne & Atteia 2009). While some GW emissions, such as from core-collapse SNe, are expected to reach frequencies up to a few kilohertz (Radice et al. 2019), we restrict our search frequency range to the most sensitive band of the GW detectors, 20–500 Hz, since detecting such signals above a few hundred hertz requires extremely high GW energies (Abbott et al. 2019b, Figure 4) and expanding the frequency range would also significantly increase the computational cost. To constrain the sky location of the GRB event, the search is using a grid based on the best localization known either from Fermi/GBM or Swift/BAT.

`X-Pipeline` produces time–frequency maps of the GW data coherently combined between the detectors. These maps give access to the temporal evolution of the spectral properties of the signal and enable the pipeline to search for clusters of pixels containing excess energy, referred to as *events*. The pipeline assigns each event a detection statistic based on energy and ranks them accordingly. A coherent consistency test, based on correlations between data in different detectors, then vetoes events that are associated with noise transients. The surviving event with the largest ranking statistic is the best candidate for a GW detection, and the search quantifies its significance as the probability of the event being produced by the background alone. This is determined by comparing the S/N of the trigger within the 660 s on-source window to the distribution of the S/Ns of the loudest triggers in the 660 s off-source windows. As a requirement, the off-source data consist of at least ∼1.5 hr of coincident data from at least two detectors around the time of a GRB. This is small enough to select data where the detectors should be in a similar state of operation as during the GRB on-source window, and large enough so that probability estimates using artificial time-shifting of the data are at the sub-percent level.

We quantify the sensitivity of the generic transient search by injecting simulated signals into off-source data. For each waveform family injected we determine the largest significance of any surviving cluster associated with the injections. We compute the percentage of injections that have a significance higher than the best event candidate and look for the amplitude at which this percentage is above 90%, which sets the upper limit. We include O3b calibration errors (Acernese et al. 2022; Sun et al. 2021) by jittering the amplitude and arrival time according to a Gaussian distribution representative of the calibration uncertainties. As with the modeled search, these injection sets allow us to calculate 90% exclusion distances.

We choose simulated waveforms to cover the search parameter space of three distinct sets of circular waveforms: BNS and NSBH binary inspiral signals, stellar collapse, and disk instability models.

1. Circular sine–Gaussian (CSG): signals representing GW emission from stellar collapses defined in Equation (1) of Abbott et al. (2017e) with a Q factor of 9 and varying center frequency of 70, 100, 150, and 300 Hz. In all cases, we assume an optimistic emission of energy in GWs of $E_{\rm GW} = 10^{-2}M_{\odot}c^2$.
2. Binary inspiral: signals are characterized by a Gaussian distribution centered at $1.4M_{\odot}$, with a width of $0.2M_{\odot}$ for an NS in a BNS, and with a width of $0.4M_{\odot}$ for an NS in an NSBH. The distribution for GWs emitted by BNS mergers addresses the case of short GRB events as in Abbott et al. (2017e) and adopted in the `PyGRB` search (Section 3.1).
3. Accretion disk instability (ADI): long-duration waveforms for GWs produced by instabilities in the magnetically suspended torus around a rapidly spinning BH. The model specifics and parameters used to generate the five families of ADI signals are the same as in the previous searches (Abbott et al. 2017e, 2019d, 2020).

In the O3a search, the sensitivity to long-duration ($\gtrsim$10 s) signals was often limited by loud background noise transients known as *glitches* (Davis et al. 2021). While `X-Pipeline`'s coherent consistency tests easily veto these glitches, many long-duration simulated signals would overlap such a glitch by chance. In these cases the simulated signal and glitch would be clustered together and subsequently vetoed together. To

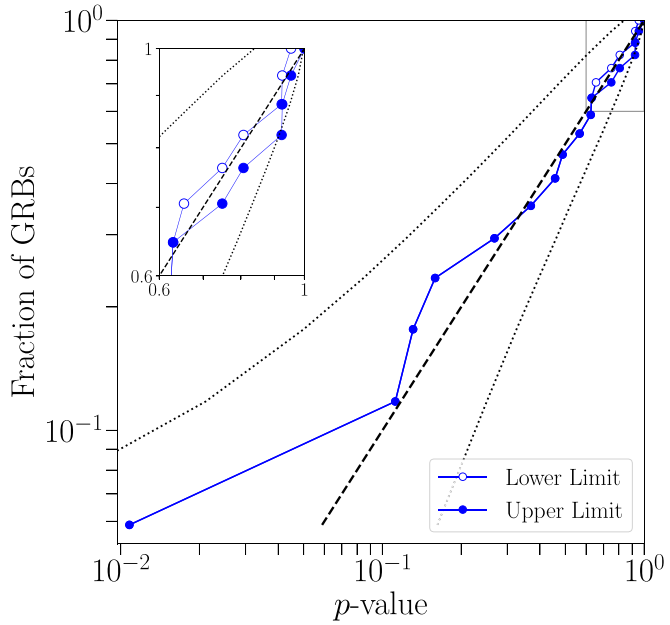

Figure 1. The cumulative distribution of p-values for the loudest on-source events for the modeled search in O3b. If a trigger is found in the on-source the upper and lower limits are identical to the reported p-value. If no trigger is identified in the on-source window, we set an upper limit on the p-value of 1, and a lower limit equal to the fraction of off-source trials that also did not contain a trigger. The upper limits are plotted as the curve with full circles and the lower limits are plotted as the curve with empty circles. The dashed line indicates an expected uniform distribution of p-values under a no-signal hypothesis, with the corresponding 90% band as the dotted lines.

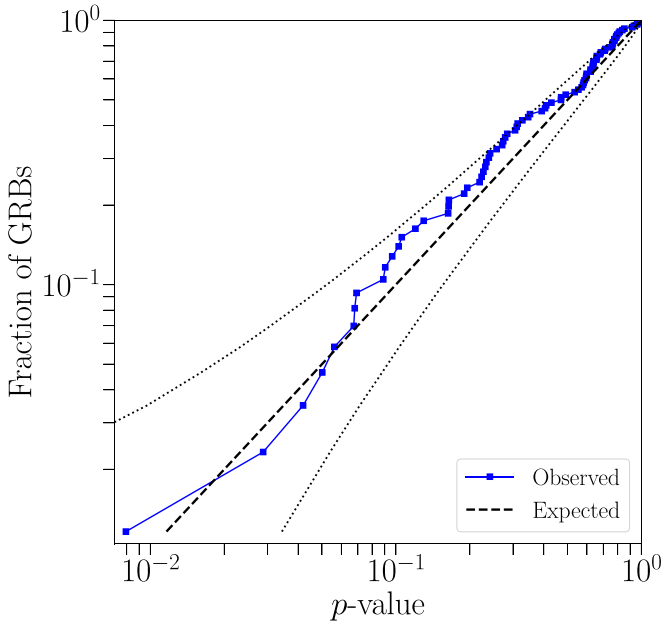

Figure 2. The cumulative distribution of p-values for the loudest on-source events for the generic transient search in O3b. Unlike with the modeled search, there is a p-value found for all GRBs analyzed by the generic transient search, so there are no upper and lower limits. The observed values are plotted as the curve with full circles. The dashed line indicates an expected uniform distribution of p-values under a no-signal hypothesis, with the corresponding 90% band as the dotted lines.

address this problem, we implemented an *autogating* procedure for O3b. For each detector, we compute the total energy in the whitened data stream over a 1 s window. If this total fluctuates by more than 50 standard deviations above the median value, then the data is zeroed out over the interval where the threshold is exceeded and we apply an inverse 1 s Tukey window at each end of the zeroed interval to transition smoothly between the whitened and zeroed data. To minimize the possibility of a loud GW transient triggering a gate, the procedure cancels a gate if there is a simultaneous energy excursion above 10 standard deviations in any other detector. The threshold of 50 standard deviations is low enough to gate the most problematic loud glitches, while being high enough that the only GWs zeroed out by the gate would have been detectable by all-sky searches. Empirically we find that this procedure is effective at reducing the impact of loud glitches without affecting the sensitivity to low-amplitude GW signals.

For both search methods, we rank each candidate by calculating a p-value, the probability of an event or a louder one in the on-source data, given the background distribution, under the null hypothesis. The p-value is calculated by counting the fraction of background trials that contain an event with a greater signal-to-noise ratio than that of the loudest on-source event.

4. Results of Analyses

We followed up on 86 GRB triggers with the generic transient method and 17 GRBs (those categorized as short or ambiguous) with the modeled search. None of the analyses indicate the presence of a statistically significant GW signal associated with one or more of the GRBs. This null result is consistent with the estimated GW–GRB joint detection rate with Fermi/GBM of 0.07–1.80 yr^{-1} reported previously in Abbott et al. (2019a) for the second observing run of Advanced LIGO and Advanced Virgo (O2).

We present the cumulative p-value distributions from both search methods in Figures 1 and 2. In these plots, a significant event would appear at a much lower p-value in the lower left corner of the plots, and be outside (to the left) of the 90% confidence region. Both plots show that the p-value distributions are consistent with the background.

The most significant event from the modeled search had a p-value of 1.08×10^{-2} (GRB 200129A). Through further investigation of this candidate event, a period of excess noise in one of the detectors was discovered ∼20 s before the candidate time. To determine the effect of this noise on the candidate, we used BayesWave to reconstruct the glitch and then clean the data by subtracting the reconstruction (Pankow et al. 2018; Cornish et al. 2021). After this cleaning, we conducted a coherent matched filtering on the cleaned data and the recovered candidate was no longer significant with respect to the background. This result suggests that much of the power of the candidate was caused by noise and not a GW. Even if there is a quiet GW at this time, it is not strong enough without the contribution from the glitch to survive ranking against the background in the analysis.

The lowest reported p-value found during O3b for the generic transient search was 7.95×10^{-3} (GRB 200224B). Although this p-value is very small, it is not unexpected given the high number of GRBs analyzed.

Given that no loud GW signals were observed coincident with any of the GRBs in either of our searches, we perform a weighted binomial test to determine the probability of observing our set of p-values assuming a uniform background distribution. A small probability would suggest that there may be a population of subthreshold GW signals that our searches

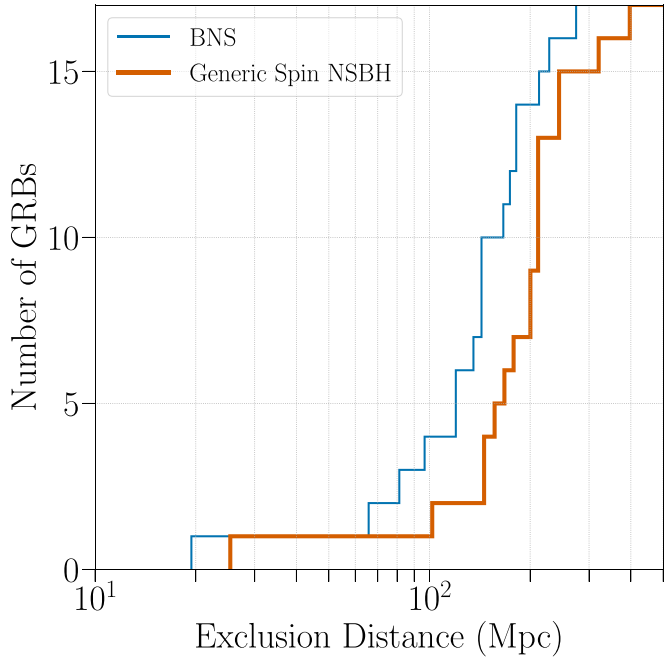

Figure 3. Cumulative histograms of the 90% exclusion distances, D_{90}, for the 17 GRBs that the modeled search followed up on in O3b. The thin blue line shows generically spinning BNS models and the thick orange line shows generically spinning NSBH models.

Table 1
Median 90% Exclusion Distances (D_{90}) for the Both the Modeled and Generic Transient Searches during O3b

Modeled Search (Short GRBs)	BNS	NSBH Generic Spins	NSBH Aligned Spins
D_{90} (Mpc)	149	207	257

Generic Transient Search (All GRBs)	CSG 70 Hz	CSG 100 Hz	CSG 150 Hz	CSG 300 Hz
D_{90} (Mpc)	166	126	92	42

Generic Transient Search (All GRBs)	ADI A	ADI B	ADI C	ADI D	ADI E
D_{90} (Mpc)	34	140	54	22	52

Note. For the modeled searches, we report the median (D_{90}) values for all three simulated signal types. For the generic search, we report results obtained with CSG (Abbott et al. 2017e) and ADI (van Putten 2001; van Putten et al. 2014) models.

did not identify. This type of weighted binomial test, fully described in the Appendix of Abadie et al. (2012), uses the lowest re-weighted p-values from the searches. The resulting probability for the modeled search is 0.07. If we remove GRB 200129A, for which the small p-value is the result of noise, the probability becomes 0.68, suggesting no population of weak GW signals. For the generic transient search, the test gives a probability of 0.76. These same weighted binomial tests carried out in O3a returned probabilities of 0.43 and 0.30 for the modeled and generic transient searches, respectively (Abbott et al. 2020). In O2 (removing GW170817/GRB 170817A) and the first observing run of Advanced LIGO and Advanced Virgo (O1) the probabilities were 0.30 and 0.75, and 0.57 and 0.75, respectively (Abbott et al. 2017e, 2019a). As in these previous analyses, the probabilities obtained in O3b suggest that no weak GWs can be attributed to the population of GRBs.

In Figure 3, we present the cumulative 90% exclusion distances for the 17 GRBs analyzed with the modeled search. The first of these 17 GRBs, GRB 200323A, has significantly lower exclusion distances than the rest. We can attribute this to the fact that the analysis of this GRB only used data from the Virgo interferometer. Furthermore, this GRB has a suboptimal sky location for the Virgo interferometer with a sensitivity, when compared to an optimal sky location, of ∼30%. Both of these factors produce the relatively small exclusion distances for the first step in the histogram. Table 1 reports the median D_{90} for the 17 GRBs analyzed with the modeled search. It shows median values for all three of the injected signal types described in Section 3.1. For comparison, all three of these median values are 10%–30% larger than those reported from the same modeled search in O3a (Abbott et al. 2020). This difference stems from having a larger fraction of GRBs in O3b that by chance arrived with better LIGO–Virgo antenna factors on average, bringing up the median values. The individual D_{90} values for each of the 17 GRBs analyzed with the modeled search can be seen in Table 2.

Similar to the modeled search, we derive a 90% confidence level lower limit on the distance for each of the 86 GRBs analyzed with the generic transient search, based on the different emission models described in Section 3.2. We present the distribution of D_{90} values for the ADI model A (van Putten 2001; van Putten et al. 2014) and for a CSG with central frequency of 150 Hz (Abbott et al. 2017e) in Figure 4. The limits reported depend on the sensitivity of the instruments in the network, which change with time and sky localization of the GRB events. We marginalize these limits over errors introduced by detector calibration. In Table 1, we report the median exclusion distance limits, D_{90}, for the set of GRBs for the different signals described in Section 3.2. The limits vary by nearly an order of magnitude due to the variety of signals used in our analysis. On average the median values for the O3b generic transient search are about 50% greater than those reported in O3a (Abbott et al. 2020). We can primarily attribute this improvement to the use of autogating in O3b: the increase in exclusion distances is highest (up to a factor of 2) for the longest-duration waveforms, which are most impacted by the glitches removed by autogating (as explained in Section 3). The exclusion distances for the shorter-duration CSG waveforms, which are not expected to be affected by autogating, increased by about 30% on average. This is more than could be accounted for by chance differences in the LIGO–Virgo antenna factors between the two samples. Rather, the increase is likely due to improvements in the performance of the detectors themselves, such as through the reduction of noise caused by scattered light in the LIGO detectors (Soni et al. 2021) or the improvement in sensitivity of the Virgo detector (Davis et al. 2021). We report the D_{90} values found for each GRB in the case of ADI model A simulated signals

Table 2
GRB Details and Associated GW Emission Limits for Each of the Fermi and Swift GRBs Followed Up On during O3b

GRB Name	UTC Time	R.A.	Decl.	Satellite	T_{90}(s)	δT_{90} (s)	D_{90} (Mpc)						
							Type	Network	BNS	Generic NSBH	Aligned NSBH	ADI-A	CSG 150 Hz
191101A	21:08:03	$16^h\ 47^m\ 25^s$	43° 45′	Swift	142.708	18.247	Long	H1L1V1[a]	…	…	…	204	72
191106A	14:15:23	$17^h57^m26^s$	46° 03′	Swift	3.436	0.325	Ambiguous	H1	71	112	148	…	…
191110A	14:05:34	$17^h\ 20^m\ 48^s$	43° 31′	Fermi	14.848	7.141	Long	H1L1V1	…	…	…	104	32
191111347	08:19:09	$8^h\ 42^m\ 09^s$	−32° 28′	Fermi	5.376	0.923	Long	H1L1	…	…	…	91	31
191111A	08:44:29	$12^h\ 37^m\ 09^s$	−32° 07′	Fermi	88.066	0.923	Long	H1L1[a]	…	…	…	102	42
191111B	13:07:10	$15^h\ 57^m\ 38^s$	−70° 25′	Fermi	158.212	7.209	Long	H1V1[a]	…	…	…	73	26
191117A	00:08:28	$19^h\ 51^m\ 31^s$	76° 23′	Fermi	7.424	1.619	Long	H1L1	…	…	…	144	54
191117B	15:17:38	$10^h\ 29^m\ 40^s$	7° 14′	Fermi	1.28	0.87	Ambiguous	H1V1	141	189	257	77	25
191118A	22:12:01	$14^h\ 15^m\ 57^s$	−48° 24′	Fermi	36.353	2.064	Long	L1V1	…	…	…	78	22
191119261	06:16:07	$20^h\ 37^m\ 24^s$	−9° 21′	Fermi	8.448	3.566	Long	H1L1	…	…	…	39	17
191122A	13:32:56	$3^h\ 37^m\ 09^s$	−32° 11′	Swift	125.736	31.050	Long	H1L1V1[a]	…	…	…	148	49
191123A	10:38:44	$14^h\ 21^m\ 10^s$	22° 50′	Swift	284.812	52.232	Long	L1V1[a]	…	…	…	105	32
191125A	04:56:43	$16^h\ 12^m\ 21^s$	−13° 07′	Fermi	77.31	0.81	Long	H1L1V1[a]	…	…	…	177	59
191125B	15:12:45	$23^h\ 34^m\ 09^s$	18° 12′	Fermi	46.336	8.208	Long	H1L1V1	…	…	…	104	35
191129A	03:22:27	$0^h\ 35^m\ 43^s$	5° 26′	Fermi	19.968	1.056	Long	L1V1	…	…	…	69	34
191130253	06:04:41	$23^h\ 17^m\ 36^s$	63° 05′	Fermi	121.09	1.45	Long	H1V1[a]	…	…	…	60	24
191130507	12:09:34	$23^h\ 14^m\ 24^s$	−7° 44′	Fermi	61.953	1.145	Long	L1V1[a]	…	…	…	74	36
191130A	13:05:02	$8^h\ 52^m\ 19^s$	4° 60′	Swift	17.56	2.88	Long	L1V1	…	…	…	95	33
191202A	20:48:51	$16^h\ 38^m\ 08^s$	17° 33′	Fermi	30.72	0.81	Long	H1L1V1	…	…	…	183	70
191203A	06:57:19	$22^h\ 09^m\ 33^s$	51° 49′	Fermi	0.83	0.64	Short	H1L1	87	153	180	73	32
191205741	17:46:20	$0^h\ 56^m\ 09^s$	−34° 09′	Fermi	2.05	3.62	Ambiguous	H1L1	189	211	355	146	58
191213254	06:05:33	$13^h\ 04^m\ 14^s$	−30° 27′	Fermi	18.944	2.919	Long	H1L1V1	…	…	…	84	50
191213B	18:49:07	$22^h\ 04^m\ 14^s$	−13° 56′	Fermi	9.216	4.615	Long	H1L1V1	…	…	…	20	9
191213A	04:06:23	$14^h\ 58^m\ 07^s$	−9° 45′	Swift	118.992	18.265	Long	H1L1V1[a]	…	…	…	39	51
191220589	14:08:29	$14^h\ 07^m\ 04^s$	−67° 31′	Fermi	27.905	1.056	Long	L1V1	…	…	…	74	22
191220A	13:29:37	$18^h\ 45^m\ 20^s$	26° 40′	Swift	175.584	125.995	Long	L1V1[a]	…	…	…	94	33
191221A	19:14:28	$2^h43^m19^s$	−43° 02′	Fermi	2.24	0.78	Ambiguous	H1V1	166	219	327	…	…
191221B	20:39:13	$10^h\ 19^m\ 19^s$	−38° 09′	Swift	48.0	16.0	Long	H1V1[a]	…	…	…	105	34
191225A	07:25:16	$6^h\ 21^m\ 57^s$	−17° 21′	Fermi	112.38	11.31	Long	L1V1[a]	…	…	…	92	32
191225B	17:37:51	$9^h\ 43^m\ 12^s$	−7° 11′	Fermi	82.69	2.92	Long	H1L1[a]	…	…	…	44	32
191227723	17:21:44	$17^h\ 12^m\ 40^s$	−26° 01′	Fermi	0.208	0.066	Short	H1L1V1	144	207	253	129	46
191227A	01:39:37	$21^h\ 16^m\ 40^s$	−16° 43′	Swift	55.888	16.282	Long	H1V1[a]	…	…	…	98	32
191228A	00:01:19	$0^h\ 21^m\ 27^s$	−8° 41′	Swift	193.816	29.875	Long	H1L1V1[a]	…	…	…	148	52
200101861	20:39:26	$17^h\ 09^m\ 43^s$	−35° 04′	Fermi	9.984	0.326	Long	L1V1	…	…	…	70	18
200103678	16:16:50	$23^h\ 41^m\ 31^s$	−38° 22′	Fermi	9.984	4.971	Long	H1V1	…	…	…	36	16
200103689	16:32:23	$7^h\ 53^m\ 55^s$	−0° 54′	Fermi	68.1	5.4	Long	H1L1V1[a]	…	…	…	27	18
200105914	21:55:28	$21^h\ 32^m\ 07^s$	−41° 11′	Fermi	16.896	2.919	Long	H1L1V1	…	…	…	74	23
200109A	01:46:16	$20^h\ 28^m\ 27^s$	52° 59′	Swift	112.0	32.0	Long	L1V1[a]	…	…	…	80	25
200110518	12:26:08	$6^h\ 24^m\ 36^s$	28° 53′	Fermi	153.859	2.064	Long	H1V1[a]	…	…	…	60	22
200112395	09:28:27	$12^h\ 27^m\ 52^s$	−34° 19′	Fermi	38.912	4.222	Long	H1L1V1	…	…	…	96	36
200112A	12:36:31	$10^h\ 00^m\ 31^s$	64° 25′	Fermi	4.925	0.602	Long	H1L1V1	…	…	…	141	45
200114A	03:40:43	$13^h\ 17^m\ 31^s$	−0° 19′	Fermi	29.69	0.81	Long	H1L1V1	…	…	…	141	48
200115A	11:50:23	$3^h\ 45^m\ 48^s$	5° 36′	Swift	242.14	27.23	Long	H1L1[a]	…	…	…	102	34
200117517	12:24:06	$8^h\ 38^m\ 40^s$	−62° 31′	Fermi	28.416	2.187	Long	H1L1V1	…	…	…	99	27
200120A	23:04:55	$9^h\ 08^m\ 32^s$	−70° 26′	Fermi	12.8	2.9	Long	H1V1	…	…	…	105	46
200122221	05:18:20	$8^h\ 18^m\ 38^s$	67° 05′	Fermi	2.816	2.673	Ambiguous	H1L1V1	183	247	371	162	41
200122A	01:41:00	$14^h\ 00^m\ 02^s$	27° 33′	Swift	190.596	4.515	Long	H1L1V1[a]	…	…	…	101	32
200125B	20:43:31	$0^h\ 29^m\ 47^s$	64° 41′	Fermi	5.824	0.091	Long	H1L1	…	…	…	176	69
200126466	11:10:51	$3^h\ 57^m\ 52^s$	−59° 37′	Fermi	0.768	1.168	Short	L1V1	149	214	300	102	23
200127B	18:11:18	$5^h\ 03^m\ 33^s$	20° 04′	Fermi	33.025	2.919	Long	H1L1	…	…	…	95	33

Table 2
(Continued)

GRB Name	UTC Time	R.A.	Decl.	Satellite	T_{90}(s)	δT_{90} (s)	D_{90} (Mpc)						
							Type	Network	BNS	Generic NSBH	Aligned NSBH	ADI-A	CSG 150 Hz
200128A	03:40:05	$10^h\ 34^m\ 36^s$	41° 34′	Fermi	0.576	0.181	Short	L1V1	149	207	253	94	27
200129A	09:48:44	$23^h\ 05^m\ 07^s$	−44° 58′	Fermi	0.112	0.464	Short	H1L1V1(H1L1)	235	323	454	203	64
200130A	05:57:16	$21^h\ 57^m09^s$	−65° 56′	Fermi	56.577	3.114	Long	H1V1	…	…	…	110	34
200130B	09:59:56	$9^h\ 10^m\ 07^s$	−51° 20′	Fermi	11.293	0.383	Long	H1L1	…	…	…	14	6
200131A	22:41:15	$0^h\ 12^m\ 21^s$	51° 07′	Swift	32.74	0.88	Long	H1L1V1	…	…	…	213	78
200201A	00:57:20	$19^h\ 10^m\ 50^s$	−11° 02′	Fermi	12.544	1.379	Long	H1L1V1	…	…	…	102	34
200205C	20:17:23	$14^h\ 52^m\ 50^s$	−42° 47′	Fermi	17.408	1.448	Long	H1L1	…	…	…	142	50
200207A	01:22:55	$16^h\ 16^m\ 21^s$	−48° 18′	Fermi	15.616	2.429	Long	L1V1	…	…	…	71	32
200208A	01:14:17	$1^h\ 46^m\ 55^s$	25° 19′	Fermi	20.992	6.931	Long	L1V1	…	…	…	95	46
200211A	07:26:28	$23^h\ 00^m\ 48^s$	−7° 09′	Fermi	78.594	0.362	Long	H1L1[a]	…	…	…	188	72
200212A	10:49:49	$8^h\ 19^m\ 11^s$	22° 57′	Fermi	10.50	1.95	Long	H1L1	…	…	…	94	34
200215A	14:39:31	$2^h\ 16^m\ 24^s$	12° 47′	Swift	11.148	2.155	Long	H1V1	…	…	…	101	33
200216A	09:07:25	$20^h\ 45^m\ 45^s$	−11° 39′	Swift	8.192	1.639	Long	H1L1V1	…	…	…	155	51
200216B	13:32:33	$10^h\ 41^m\ 49^s$	19° 28′	Swift	67.448	6.568	Long	H1L1V1[a]	…	…	…	93	33
200219B	09:54:14	$19^h\ 56^m\ 31^s$	6° 39′	Fermi	9.984	1.305	Long	H1L1V1	…	…	…	122	46
200219A	07:36:49	$22^h\ 50^m\ 22^s$	−59° 06′	Swift	288.0	50.6	Long	H1L1V1[a]	…	…	…	215	76
200221A	03:52:58	$10^h\ 28^m\ 24^s$	33° 08′	Fermi	1.728	1.336	Ambiguous	H1L1V1	213	247	377	152	55
200223A	19:32:03	$16^h\ 33^m\ 33^s$	−55° 47′	Fermi	65.281	10.555	Long	L1V1[a]	…	…	…	102	33
200224B	05:05:49	$11^h\ 51^m\ 36^s$	−28° 52′	Fermi	299.525	2.862	Long	H1L1V1[a]	…	…	…	94	34
200224C	09:58:44	$12^h\ 28^m\ 04^s$	−19° 33′	Fermi	0.064	1.922	Short	H1L1V1	120	160	220	112	33
200224A	03:24:49	$16^h\ 34^m\ 58^s$	41° 40′	Swift	45.0	9.2	Long	H1L1	…	…	…	10	7
200227A	07:20:08	$3^h\ 45^m\ 43^s$	9° 29′	Swift	30.328	9.202	Long	H1L1V1	…	…	…	69	21
200228A	06:58:33	$21^h\ 52^m\ 02^s$	−46° 27′	Fermi	3.584	0.345	Ambiguous	H1L1V1(H1L1)	282	399	528	231	76
200228B	11:14:41	$16^h\ 48^m\ 01^s$	16° 58′	Swift	7.368	1.576	Long	H1L1	…	…	…	203	73
200301320	07:40:46	$21^h\ 20^m\ 33^s$	7° 30′	Fermi	18.176	1.145	Long	H1L1V1	…	…	…	155	48
200303A	02:34:57	$14^h\ 10^m\ 47^s$	51° 22′	Swift	94.22	6.40	Long	H1L1V1[a]	…	…	…	100	30
200306B	22:25:25	$23^h\ 18^m\ 07^s$	5° 06′	Fermi	0.992	1.226	Ambiguous	L1V1	98	156	221	28	19
200306C	22:50:39	$13^h\ 14^m\ 18^s$	11° 16′	Swift	53.152	13.725	Long	L1V1[a]	…	…	…	101	32
200307A	21:26:59	$5^h\ 36^m\ 43^s$	−46° 13′	Fermi	1.664	0.659	Ambiguous	H1L1(H1L1V1)	121	172	195	96	34
200308A	22:35:15	$21^h\ 49^m\ 45^s$	−27° 45′	Fermi	43.01	2.56	Long	H1L1V1	…	…	…	124	39
200311A	15:16:12	$13^h\ 35^m\ 57^s$	−49° 41′	Fermi	52.48	0.81	Long	H1L1	…	…	…	133	49
200313A	01:41:36	$5^h\ 03^m\ 09^s$	20° 53′	Fermi	13.568	0.572	Long	H1L1V1	…	…	…	210	73
200313B	10:57:12	$13^h28^m41^s$	40° 30′	Fermi	5.184	4.362	Ambiguous	L1V1	181	219	286	…	…
200317A	00:40:30	$4^h\ 22^m\ 09^s$	−46° 19′	Fermi	7.616	0.529	Long	H1L1V1	…	…	…	54	16
200319A	07:44:40	$4^h\ 21^m\ 09^s$	−21° 15′	Fermi	20.48	3.17	Long	H1L1	…	…	…	137	47
200320A	09:56:46	$12^h\ 17^m\ 21^s$	−38° 44′	Fermi	9.021	1.072	Long	H1L1V1	…	…	…	44	15
200323006	00:08:42	$22^h\ 56^m\ 50^s$	53° 02′	Fermi	7.168	2.521	Long	L1V1	…	…	…	62	17
200323A	18:46:32	$10^h25^m53^s$	−55° 32′	Fermi	2.11	0.58	Ambiguous	V1	19	25	38	…	…
200326A	12:24:47	$16^h\ 21^m\ 19^s$	−21° 05′	Fermi	96.512	4.419	Long	H1L1V1[a]	…	…	…	104	33

Notes. The GRB Name column reports each GRB's formal designation (Barthelmy et al. 2009) or the Fermi GBM trigger ID when a formal designation has not been assigned. The UTC times reported are rounded to the earlier integer second. The Satellite column gives the satellite that provided the GRB sky localization used in the GW analysis. The Network column lists the GW detector network used: H1 = LIGO Hanford, L1 = LIGO Livingston, V1 = Virgo.

[a] The symbol indicates that the GRB's $T_{90} > 60$ s, so the generic transient search's on-source window was extended. Where the generic transient search (Section 3.2) and the modeled search (Section 3.1) used a different IFO network, the network used by the modeled search is shown in parentheses. The last five columns show the 90% confidence exclusion distances for each GRB (D_{90}) for the following emission scenarios: BNS, generic, and aligned-spin NSBH from the modeled search, and from the generic transient search, ADI-A and CSG GW burst at 150 HZ with total radiated energy $E_{GW} = 10^{-2}\, M_\odot\, c^2$.

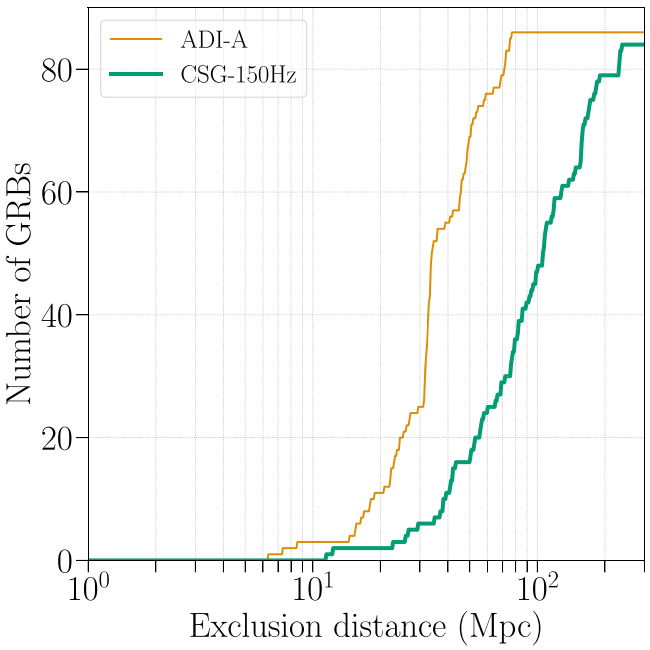

Figure 4. Cumulative histograms of the 90% confidence exclusion distances, D_{90}, for the ADI signal model A (orange, thin line) and the CSG 150 Hz model (green, thick line). For a given GRB and signal model, this is the distance within which 90% of simulated signals inserted into off-source data are successfully recovered with a significance greater than the loudest on-source trigger.

and CSG simulated signals with a central frequency of 150 Hz in Table 2, at the end of this paper.

5. Population Studies

We use the results obtained from the GW follow-up analysis of GRBs to put constraints on the low-luminosity short GRB population. For this purpose, we describe the short GRB population through a simple luminosity function model following (Wanderman & Piran 2015), extended at low luminosities following the procedure described in (Abbott et al. 2019d). We can then model the luminosity distribution through a power law with two breaks

$$\phi_0(L_{\rm iso}) \equiv \frac{dP}{d\log(L_{\rm iso})} = \begin{cases} \left(\frac{L_{\rm iso}}{L_{**}}\right)^{-\gamma_L}\left(\frac{L_{**}}{L_*}\right)^{-\alpha_L}, & L_0 \leqslant L_{\rm iso} \leqslant L_{**} \\ \left(\frac{L_{\rm iso}}{L_*}\right)^{-\alpha_L}, & L_{**} < L_{\rm iso} \leqslant L_*\,, \\ \left(\frac{L_{\rm iso}}{L_*}\right)^{-\beta_L}, & L_{\rm iso} > L_* \end{cases} \quad (1)$$

where $L_{\rm iso}$ is the isotropic equivalent GRB luminosity and for which we have $L_* = 2\times10^{52}$ erg s^{-1}, $L_{**} = 5\times10^{49}$ erg s^{-1}, $\alpha_L = 0.94$, and $\beta_L = 2$ (Wanderman & Piran 2015). We do not take into account the measurement uncertainties for those fixed parameters as they would not significantly influence the analysis. The parameters on which we aim to put constraints using the joint GW–GRB analysis are the low-luminosity power index γ_L and the low-luminosity cutoff for our population L_0. To make the dependence from these parameters clearer, we refer to the luminosity distribution as $\phi_0(L_{\rm iso}) \equiv \phi_0(L_{\rm iso}, \gamma_L, L_0)$. A Bayesian analysis constrains the parameters γ_L and L_0 using the results from the O1, O2, O3a, and O3b `PyGRB` searches (Harry & Fairhurst 2011; Williamson et al. 2014; Abbott et al. 2019d, 2020) and the results on BNS rates from Abbott et al. (2021c).

Under certain conditions, NSBH mergers can also produce short GRBs (Narayan et al. 1992) and a small fraction of short GRBs can arise from local magnetar giant flares (Burns et al. 2021). For simplicity, we ignore those relatively uncommon possibilities here. We assume that BNS coalescences are the only progenitors for short GRBs, since there are restricted conditions under which an NSBH coalescence results into a short GRB (Pannarale & Ohme 2014).

First, we compute the observed cumulative rate distribution $C_R^{\rm obs}(z, \gamma_L, L_0)$ as a function of redshift z, γ_L, and L_0. To do so, we take into account the cosmic rate density for short GRB explosions $\psi(z)$ adopting its form given in Wanderman & Piran (2015). A Band function models the energy spectrum of the short GRBs (Band et al. 1993) with power indices $\alpha_{\rm Band} = -0.5$, $\beta_{\rm Band} = -2.25$ and peak energy $E_{\rm peak} = 800$ keV, and we use Equation (1) as the luminosity distribution function for our population of short GRBs. As in Wanderman & Piran (2015), we consider short GRBs detectable in gamma-rays when their 64 ms peak photon flux is above $P_{64}^{\rm th} = 2.37$ photons cm^{-2} s^{-1} in the energy window considered for Fermi/GBM, i.e., [50–300] keV. We then compute the cumulative observed rate distribution as

$$C_R^{\rm obs}(z, \gamma_L, L_0) = \int_0^z \frac{dP_{\rm obs}^{\rm GRB}}{dz'} dz', \quad (2)$$

where the differential probability of having an observed short GRB is defined as

$$\frac{dP_{\rm obs}^{\rm GRB}}{dz} \propto \frac{\psi(z)}{(1+z)}\frac{dV}{dz}\epsilon(z, \gamma_L, L_0)\,. \quad (3)$$

Here in Equation (3), $\psi(z)$ is the short GRB redshift distribution, dV/dz is the differential comoving volume and $\epsilon(z, \gamma_L, L_0)$ is the fraction of short GRBs bright enough to be detected by Fermi/GBM as a function of redshift and of the low-luminosity parameters of the luminosity distribution.

Starting from $C_R^{\rm obs}(z, \gamma_L, L_0)$, an uninformative prior probability density function (PDF) $\Pi_u(\gamma_L, L_0)$ is built considering a flat probability distribution in the logarithms of the local observed rate density and of L_0. We then impose the total local short GRB rate to have the local BNS rate as an upper limit: using the inferred BNS local rate density $\mathcal{P}_{\rm BNS}(R_0^{\rm BNS})$ (Abbott et al. 2021c) we define

$$\mathfrak{f}(\gamma_L, L_0) = \int_0^{R_0^{\rm GRB}(\gamma_L, L_0)} \mathcal{P}_{\rm BNS}(R_0'^{\rm BNS}) dR_0'^{\rm BNS}\,. \quad (4)$$

Here, $R_0^{\rm GRB}(\gamma_L, L_0)$ is the short GRB local rate density, calculated using Equation (1) as luminosity distribution, and normalized requiring consistency with the observed short GRB rate and with the analysis done by Wanderman & Piran (2015), i.e., considering the part of the population with $L_{\rm iso} > L_{**}$ to have a local rate density of 4.1 Gpc^{-3} s^{-1}. Our final,

informative prior is then defined as

$$\Pi(\gamma_L, L_0) = (1 - \mathfrak{f}(\gamma_L, L_0))\Pi_u(\gamma_L, L_0)\,. \tag{5}$$

We define the likelihood function $\mathfrak{L}(x|\gamma_L, L_0)$ (where x indicates our set of data) as the probability of detecting no GW transients associated with short or ambiguous GRBs during O1, O3a, and O3b and of detecting one single GW transient associated with a GRB observed during the O2 run. Furthermore, we impose that the joint detection occurred at the redshift measured for NGC 4993, the host galaxy of the event GW170817 ($z_{\rm NGC4993} = 0.009783$; Levan et al. 2017) and that the luminosity of the corresponding GRB is in the luminosity range measured for GRB 170817A $L_{\rm GRB\,170817A} = (1.6 \pm 0.6) \times 10^{47}$ erg s^{-1} (Abbott et al. 2017a). For our purpose we use the set of GW efficiency curves computed through the PyGRB analysis of the short and ambiguous GRBs events detected during the O1, O2, O3a, and O3b runs (respectively 20, 41, 32, and 17 events analyzed).[299]

Given a detected GRB i during O2, we compute the probability of a joint GW detection like the one observed during this run

$$P_i^{det}(\gamma_L, L_0) = \int_0^\infty \phi_0(L, \gamma_L, L_0) \ln \mathcal{N}_{\tilde{L}}(L) d\ln L \times \int_0^\infty \eta_i(z) \frac{dP_{\rm obs}^{\rm GRB}}{dz} \delta(z - z_{\rm NGC\,4993}) dz\,. \tag{6}$$

Here, $\eta_i(z)$ is the efficiency curve corresponding to the given GRB and $dP_{\rm obs}^{\rm GRB}/dz$ has been defined in Equation (3). In order to set the joint detection to have the same luminosity of GRB 170817A and the same redshift of GW170817, we choose $\mathcal{N}_{\tilde{L}}(L)$ to be a log-normal distribution with mean $L_{\rm GRB170817A} = \tilde{L}$ with $\sigma_{\tilde{L}}$ being the error on the measurement of $\tilde{L}$, and we use a Dirac delta distribution $\delta(z - z_{\rm NGC4993})$ because our analysis is insensitive to small variations in the assumed redshift.

Analogously, we can compute the probability of not having a joint GW detection associated to a given GRB detected during one of the observing runs

$$P_i^{\rm no\ det}(\gamma_L, L_0) = 1 - \int_0^\infty \eta_i(z) \frac{dP_{\rm obs}^{\rm GRB}}{dz} dz\,. \tag{7}$$

We then obtain that the probability of a single joint detection during O2 is

$$\boldsymbol{P}_{\rm O2}(\gamma_L, L_0) = \sum_i^{N_{\rm O2}^{\rm GRB}} \left(P_i^{det}(\gamma_L, L_0) \prod_{j\neq i} P_j^{\rm no\ det}(\gamma_L, L_0)\right) \tag{8}$$

while the probability of not having a joint detection during O1, O3a, and O3b is

$$\boldsymbol{P}_{\rm O1+O3}(\gamma_L, L_0) = \prod_i^{N_{\rm O1}^{\rm GRB}} P_i^{\rm no\ det}(\gamma_L, L_0) \prod_i^{N_{\rm O3}^{\rm GRB}} P_i^{\rm no\ det}(\gamma_L, L_0), \tag{9}$$

[299] There are actually 42 efficiency curves available from the O2 PyGRB analysis, but the efficiency curve corresponding to GRB 170817A was not computed properly since the pipeline considered the GW170817 event as a background event.

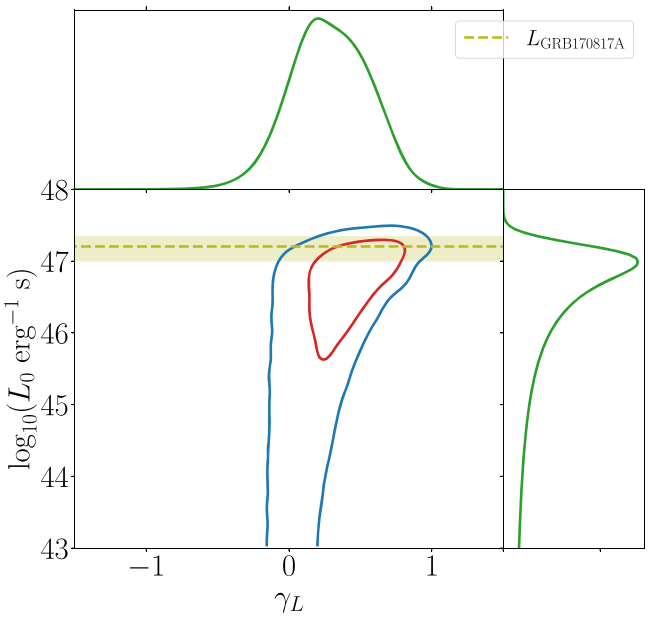

Figure 5. Contour plot of the two-dimensional posterior as a function of the γ_L parameter (horizontal axis) and of the base 10 logarithm of L_0 (vertical axis) with plots of the corresponding marginalized posterior curves (in green). The contours correspond to the 90% and 50% credible regions (respectively in blue and red) for the two parameters. The bounds regions for those two parameters are compatible with the measured luminosity from GRB 170817A (yellow dashed line with shaded area) as its value is greater than L_0 for the bulk of the values inside the regions. The marginalized posterior for L_0 peaks around $L = L_{\rm GRB170817A}$ because of the likelihood factor, which requires that the joint detection happened around that value.

then the obtained likelihood is

$$\mathfrak{L}(x|\gamma_L, L_0) = \boldsymbol{P}_{\rm O2}(\gamma_L, L_0)\boldsymbol{P}_{\rm O1+O3}(\gamma_L, L_0)\,. \tag{10}$$

Finally, we compute the posterior $P(\gamma_L, L_0|x) \propto \mathfrak{L}(x|\gamma_L, L_0)\,\Pi(\gamma_L, L_0)$, the contour plot for which is shown on Figure 5, with contours in blue and red corresponding, respectively, to the posterior 90% and 50% credible regions. The constant rate curves shape the posterior: if we fix a value of the rate, higher values for the low-luminosity cutoff L_0 favor higher values of the low-luminosity power index γ_L. Each credible region's L_0 value is compatible with the luminosity value range of GRB 170817A. Finally, the 90% credible region curve does not close for low values of L_0: this is due to the fact that we do not have any information about events down to those luminosities and for this reason we did not explore lower values for L_0. By marginalizing the posterior PDF over L_0, we obtain that $\gamma_L = 0.28 \pm 0.45$.

To present these results in the luminosity function space, we compute the rate curves $dR_0/d\log_{10}L$ for pairs of values (γ_L, L_0) sampled according to the posterior distribution $P(\gamma_L, L_0|x)$. From this set of curves we obtain the median and credible intervals on the luminosity distribution.

The plot in the top panel of Figure 6 shows the $dR_0/d\log_{10}L$ 90% and 50% credible intervals as functions of $\log_{10}L$ and compares them to other estimations performed in other works (Ghirlanda et al. 2016; Salafia et al. 2020; Tan & Yu 2020). It illustrates how the short GRB luminosity function in our model peaks around $L \sim L_{\rm GRB\,170817A}$, considering this the only short GRB event observed at such a low luminosity.

The plot in the bottom panel of Figure 6 shows the inverse cumulative short GRB rate density distribution $R_0(>L)$ as a

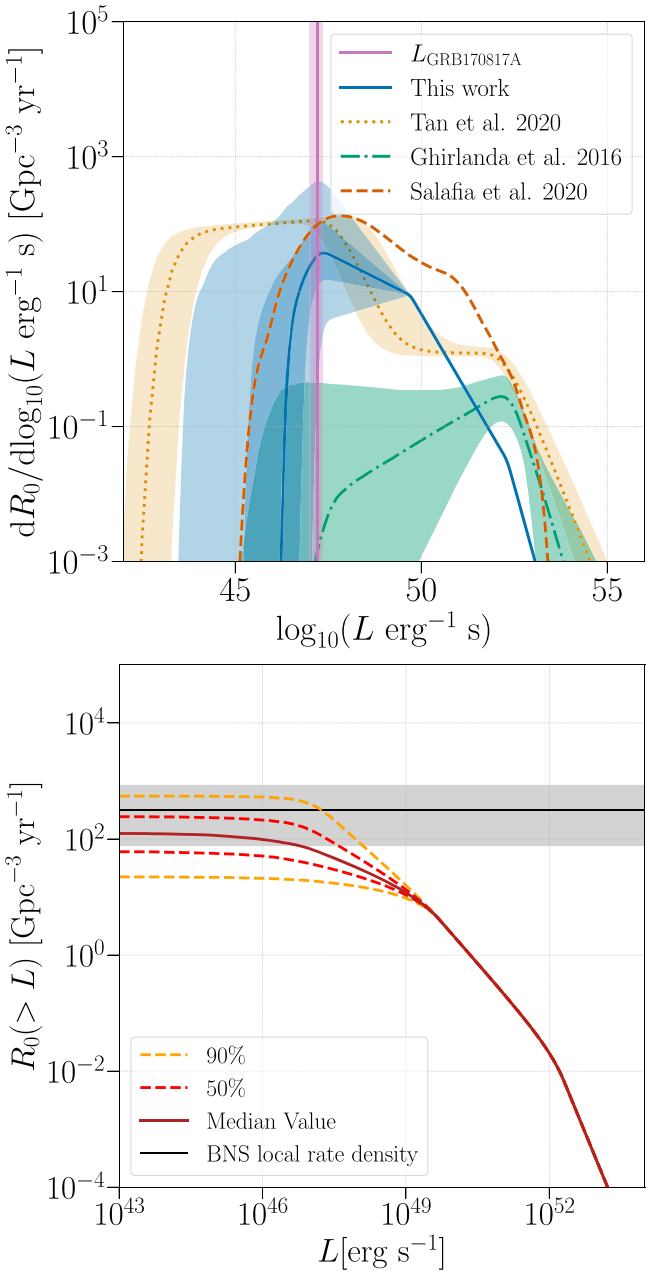

Figure 6. Plots of differential local rate densities as functions of luminosity (upper panel) and of the inverse cumulative rate density as a function of L (lower panel). In the upper plot, our set of curves is represented with the blue solid line (the solid line represents the median one and the shaded areas represent the 90% and 50% credible intervals). At large luminosity, we do not represent the error bars, since in this analysis the parameters of the distribution above $L_{**} = 5 \times 10^{49}$ erg s^{-1} were set by the analysis from Wanderman & Piran (2015). In the same plot we also show the luminosity functions from Salafia et al. (2020) (orange, dashed line), Tan & Yu (2020) (yellow, dotted line), and Ghirlanda et al. (2016) (green, dashed–dotted line). In the bottom plot we represent the median curve as a continuous brown line and the 90% and 50% credible intervals, respectively, as yellow and red dashed lines.

function of the luminosity L. The credible intervals corresponding to the sampled curve are compatible with the BNS rate density measured for Abbott et al. (2021c).

Given the present results on the low-luminosity short GRB population and the expected sensitivity for the fourth observing run of Advanced LIGO and Advanced Virgo (O4; Abbott et al. 2020), and only considering short GRBs detected by Fermi/GBM as onboard triggers, we estimate a joint GW–GRB detection rate of $R^{\rm O4}_{\rm GW-GRB} = 1.04^{+0.26}_{-0.27}$ yr^{-1} during the next data collecting period.

6. Conclusions

We followed up on Fermi/GBM and Swift/BAT GRBs reported during LIGO–Virgo's O3b and performed a targeted search using the times of the GRBs and their sky localizations to search for possible GW associations. For GRBs flagged as either short or ambiguous (see Section 2), we ran a template-based search for BNS and NSBH waveforms (Harry & Fairhurst 2011; Williamson et al. 2014). We also ran on all GRBs a generic transient analysis to look for GW signals (Sutton et al. 2010; Was et al. 2012). We did not find any significant GW candidate in coincidence with the GRBs we analyzed. Our results are consistent with the previously predicted detection rate of 0.07–1.8 yr^{-1} for O3 (Abbott et al. 2019a). We also performed a weighted binomial test to search for a population of subthreshold GW signals in our sample. We did not find strong evidence for any such event. We used different emission models to put a lower bound on the distances of the GRB progenitors. The 90% exclusion distances are reported in Table 2 for all the GRBs in our sample, along with timing and localization information as well as information on detectors used in the analyses. Finally, we performed a population study for all GRBs analyzed with the modeled search in O1 (Abbott et al. 2017e), O2 (Abbott et al. 2019a), O3a (Abbott et al. 2020), and O3b. Starting from a broken power law to model our population and constraining two of its parameters through Bayesian inference, we found that our luminosity function peaks around the luminosity value measured for GRB 170817A with this model. Furthermore, the local rate density for short GRBs is compatible with that of BNS events. Based on the present population study, we provided an estimate of the joint GW–GRB detection rate for the O4 run.

This material is based upon work supported by NSF's LIGO Laboratory, which is a major facility fully funded by the National Science Foundation. The authors also gratefully acknowledge the support of the Science and Technology Facilities Council (STFC) of the United Kingdom, the Max-Planck-Society (MPS), and the State of Niedersachsen/Germany for support of the construction of Advanced LIGO and the construction and operation of the GEO600 detector. Additional support for Advanced LIGO was provided by the Australian Research Council. The authors gratefully acknowledge the Italian Istituto Nazionale di Fisica Nucleare (INFN), the French Centre National de la Recherche Scientifique (CNRS), and the Netherlands Organization for Scientific Research (NWO), for the construction and operation of the Virgo detector and the creation and support of the EGO consortium. The authors also gratefully acknowledge research support from these agencies as well as by the Council of Scientific and Industrial Research of India, the Department of Science and Technology, India, the Science & Engineering Research Board (SERB), India, the Ministry of Human Resource Development, India, the Spanish Agencia Estatal de Investigación (AEI), the Spanish Ministerio de Ciencia e Innovación and Ministerio de Universidades, the Conselleria de Fons Europeus, Universitat i Cultura and the Direcció General de Política Universitaria i Recerca del Govern de les Illes

Balears, the Conselleria d'Innovació Universitats, Ciència i Societat Digital de la Generalitat Valenciana and the CERCA Programme Generalitat de Catalunya, Spain, the National Science Centre of Poland and the European Union—European Regional Development Fund; Foundation for Polish Science (FNP), the Swiss National Science Foundation (SNSF), the Russian Foundation for Basic Research, the Russian Science Foundation, the European Commission, the European Social Funds (ESF), the European Regional Development Funds (ERDF), the Royal Society, the Scottish Funding Council, the Scottish Universities Physics Alliance, the Hungarian Scientific Research Fund (OTKA), the French Lyon Institute of Origins (LIO), the Belgian Fonds de la Recherche Scientifique (FRS-FNRS), Actions de Recherche Concertées (ARC) and Fonds Wetenschappelijk Onderzoek—Vlaanderen (FWO), Belgium, the Paris Île-de-France Region, the National Research, Development and Innovation Office Hungary (NKFIH), the National Research Foundation of Korea, the Natural Science and Engineering Research Council Canada, Canadian Foundation for Innovation (CFI), the Brazilian Ministry of Science, Technology, and Innovations, the International Center for Theoretical Physics South American Institute for Fundamental Research (ICTP-SAIFR), the Research Grants Council of Hong Kong, the National Natural Science Foundation of China (NSFC), the Leverhulme Trust, the Research Corporation, the Ministry of Science and Technology (MOST), Taiwan, the United States Department of Energy, and the Kavli Foundation. The authors gratefully acknowledge the support of the NSF, STFC, INFN, and CNRS for provision of computational resources.

This work was supported by MEXT, JSPS Leading-edge Research Infrastructure Program, JSPS Grant-in-Aid for Specially Promoted Research 26000005, JSPS Grant-in-Aid for Scientific Research on Innovative Areas 2905: JP17H06358, JP17H06361, and JP17H06364, JSPS Core-to-Core Program A. Advanced Research Networks, JSPS Grant-in-Aid for Scientific Research (S) 17H06133 and 20H05639 , JSPS Grant-in-Aid for Transformative Research Areas (A) 20A203: JP20H05854, the joint research program of the Institute for Cosmic Ray Research, University of Tokyo, National Research Foundation (NRF) and Computing Infrastructure Project of KISTI-GSDC in Korea, Academia Sinica (AS), AS Grid Center (ASGC) and the Ministry of Science and Technology (MoST) in Taiwan under grants including AS-CDA-105-M06, Advanced Technology Center (ATC) of NAOJ, Mechanical Engineering Center of KEK.

We would like to thank all of the essential workers who put their health at risk during the COVID-19 pandemic, without whom we would not have been able to complete this work.

ORCID iDs

S. Anand https://orcid.org/0000-0003-3768-7515
I. Bartos https://orcid.org/0000-0001-5607-3637
M. W. Coughlin https://orcid.org/0000-0002-8262-2924
A. Cumming https://orcid.org/0000-0002-6335-0169
R. C. Essick https://orcid.org/0000-0001-8196-9267
A. M. Farah https://orcid.org/0000-0002-6121-0285
W. M. Farr https://orcid.org/0000-0003-1540-8562
M. Fishbach https://orcid.org/0000-0002-1980-5293
S. Galaudage https://orcid.org/0000-0002-1819-0215
Archisman Ghosh https://orcid.org/0000-0003-0423-3533
V. Granata https://orcid.org/0000-0002-1425-4541
Anuradha Gupta https://orcid.org/0000-0002-5441-9013
K. Hattori https://orcid.org/0000-0001-9933-0023
H. Hayakawa https://orcid.org/0000-0001-5370-3365
D. E. Holz https://orcid.org/0000-0002-0175-5064
K. Inayoshi https://orcid.org/0000-0001-9840-4959
P. Koch https://orcid.org/0000-0003-2777-5861
A. K. H. Kong https://orcid.org/0000-0002-5105-344X
N. Leroy https://orcid.org/0000-0002-2321-1017
S. Márka https://orcid.org/0000-0002-3957-1324
S. Nissanke https://orcid.org/0000-0001-6573-7773
F. Ricci https://orcid.org/0000-0001-5742-5980
M. Shikauchi https://orcid.org/0000-0002-3561-8658
L. P. Singer https://orcid.org/0000-0001-9898-5597
C. Talbot https://orcid.org/0000-0003-2053-5582
S. Wu https://orcid.org/0000-0002-3524-1483

References

Abadie, J., Abbott, B. P., Abbott, R., et al. 2012, ApJ, 760, 12
Abbott, B. P., Abbott, R., Abbott, T. D., et al. 2017a, ApJL, 848, L13
Abbott, B. P., Abbott, R., Abbott, T. D., et al. 2017b, ApJ, 848, L13
Abbott, B. P., Abbott, R., Abbott, T. D., et al. 2017c, PhRvL, 119, 161101
Abbott, B. P., Abbott, R., Abbott, T. D., et al. 2017d, ApJL, 848, L12
Abbott, B. P., Abbott, R., Abbott, T. D., et al. 2017e, ApJ, 841, 89
Abbott, B. P., Abbott, R., Abbott, T. D., et al. 2019a, ApJ, 886, 75
Abbott, B. P., Abbott, R., Abbott, T. D., et al. 2019b, PhRvD, 100, 024017
Abbott, B. P., Abbott, R., Abbott, T. D., et al. 2019c, PhRevX, 9, 011001
Abbott, B. P., Abbott, R., Abbott, T. D., et al. 2019d, ApJ, 886, 75
Abbott, B. P., Abbott, R., Abbott, T. D., et al. 2020, PhRvD, 101, 084002
Abbott, B. P., Abbott, R., Abbott, T. D., et al. 2020, LRR, 23, 3
Abbott, R., Abbott, T. D., Abraham, S., et al. 2020, ApJ, 915, 86
Abbott, R., Abbott, T. D., Abraham, S., et al. 2021b, ApJL, 915, L5
Abbott, R., Abbott, T. D., Abraham, S., et al. 2021c, ApJL, 913, L7
Abbott, R., Abbott, T. D., Acernese, F., et al. 2021a, arXiv:2111.03606
Acernese, F., Agathos, M., Ain, A., et al. 2022, CQG, 39, 045006
Aloy, M. A., Müller, E., Ibáñez, J. M., Martí, J. M., & MacFadyen, A. 2000, ApJL, 531, L119
Apostolatos, T. A. 1995, PhRvD, 52, 605
Arun, K. G., Buonanno, A., Faye, G., & Ochsner, E. 2009, PhRvD, 79, 104023
Babak, S., Taracchini, A., & Buonanno, A. 2017, PhRvD, 95, 024010
Band, D., Matteson, J., Ford, L., et al. 1993, ApJ, 413, 281
Barthelmy, S. D., Barbier, L. M., Cummings, J. R., et al. 2005, SSRv, 120, 143
Barthelmy, S. D., Gehrels, N., Paciesas, W., et al. 2009, GCN Circ., 10251, 1
Blanchet, L., Iyer, B. R., Will, C. M., & Wiseman, A. G. 1996, CQGra, 13, 575
Bohé, A., Faye, G., Marsat, S., & Porter, E. K. 2015, CQGra, 32, 195010
Bohé, A., Marsat, S., & Blanchet, L. 2013, CQGra, 30, 135009
Brown, D. A., Harry, I., Lundgren, A., & Nitz, A. H. 2012, PhRvD, 86, 084017
Burgay, M., D'Amico, N., Possenti, A., et al. 2003, Natur, 426, 531
Burlon, D., Ghirlanda, G., Ghisellini, G., Greiner, J., & Celotti, A. 2009, A&A, 505, 569
Burlon, D., Ghirlanda, G., Ghisellini, G., et al. 2008, ApJL, 685, L19
Burns, E., Svinkin, D., Hurley, K., et al. 2021, ApJL, 907, L28
Capano, C., Harry, I., Privitera, S., & Buonanno, A. 2016, PhRvD, 93, 124007
Cornish, N. J., Littenberg, T. B., Bécsy, B., et al. 2021, PhRvD, 103, 044006
Corsi, A., & Mészáros, P. 2009, ApJ, 702, 1171
Coyne, R. 2015, PhD thesis, The George Washington University
Dai, Z. G., & Lu, T. 1998, A&A, 333, L87
D'Avanzo, P., Campana, S., Salafia, O. S., et al. 2018, A&A, 613, L1
Davis, D., Areeda, J. S., Berger, B. K., et al. 2021, CQG, 38, 135014
Eichler, D., Livio, M., Piran, T., & Schramm, D. N. 1989, Natur, 340, 126
Fryer, C. L., Holz, D. E., & Hughes, S. A. 2002, ApJ, 565, 430
Galama, T. J., Vreeswijk, P. M., van Paradijs, J., et al. 1998, Natur, 395, 670
Gehrels, N., Chincarini, G., Giommi, P., et al. 2004, ApJ, 611, 1005
Ghirlanda, G., Salafia, O. S., Paragi, Z., et al. 2019, Sci, 363, 968
Ghirlanda, G., Salafia, O. S., Pescalli, A., et al. 2016, A&A, 594, A84
Goldstein, A., Veres, P., Burns, E., et al. 2017, ApJL, 848, L14
Gossan, S. E., Sutton, P., Stuver, A., et al. 2016, PhRvD, 93, 042002

Haggard, D., Nynka, M., Ruan, J. J., et al. 2017, ApJL, 848, L25
Hallinan, G., Corsi, A., Mooley, K. P., et al. 2017, Sci, 358, 1579
Harry, I. W., & Fairhurst, S. 2011, PhRvD, 83, 084002
Harry, I. W., Fairhurst, S., & Sathyaprakash, B. S. 2008, CQGra, 25, 184027
Harry, I. W., Nitz, A. H., Brown, D. A., et al. 2014, PhRvD, 89, 024010
Hessels, J. W. T., Ransom, S. M., Stairs, I. H., et al. 2006, Sci, 311, 1901
Hjorth, J., Sollerman, J., Møller, P., et al. 2003, Natur, 423, 847
Husa, S., Khan, S., Hannam, M., et al. 2016, PhRvD, 93, 044006
Kalogera, V., & Baym, G. 1996, ApJL, 470, L61
Khan, S., Husa, S., Hannam, M., et al. 2016, PhRvD, 93, 044007
Koshut, T. M., Kouveliotou, C., Paciesas, W. S., et al. 1995, ApJ, 452, 145
Kotake, K., Sato, K., & Takahashi, K. 2006, RPPh, 69, 971
Kouveliotou, C., Meegan, C. A., Fishman, G. J., et al. 1993, ApJL, 413, L101
Kuin, N. P. M. & Swift/UVOT Team 2019, GCN Circ., 26538, 1
Kumar, P., & Zhang, B. 2015, PhR, 561, 1
Lamb, G. P., Mandel, I., & Resmi, L. 2018, MNRAS, 481, 2581
Lazzati, D. 2005, MNRAS, 357, 722
Lazzati, D., Morsony, B. J., & Begelman, M. C. 2009, ApJL, 700, L47
Lee, W. H., & Ramirez-Ruiz, E. 2007, NJPh, 9, 17
Levan, A. J., Lyman, J. D., Tanvir, N. R., et al. 2017, ApJ, 848, L28
LIGO Scientific Collaboration 2018, LIGO Algorithm Library, doi:10.7935/GT1W-FZ16
Lyman, J. D., Lamb, G. P., Levan, A. J., et al. 2018, NatAs, 2, 751
MacFadyen, A. I., Woosley, S. E., & Heger, A. 2001, ApJ, 550, 410
Meegan, C., Lichti, G., Bhat, P. N., et al. 2009, ApJ, 702, 791
Mikoczi, B., Vasuth, M., & Gergely, L. A. 2005, PhRvD, 71, 124043
Miller, M. C., & Miller, J. M. 2014, PhR, 548, 1
Mishra, C. K., Kela, A., Arun, K. G., & Faye, G. 2016, PhRvD, 93, 084054
Mooley, K. P., Deller, A. T., Gottlieb, O., et al. 2018, Natur, 561, 355
Narayan, R., Paczynski, B., & Piran, T. 1992, ApJL, 395, L83
Neill, D., Tsang, D., van Eerten, H., Ryan, G., & Newton, W. G. 2021, MNRAS, in press, arXiv:2111.03686
Nitz, A., Harry, I., Brown, D., et al. 2020, gwastro/pycbc: PyCBC, Zenodo, doi:10.5281/zenodo.3961510
Norris, J. P., & Bonnell, J. T. 2006, ApJ, 643, 266
Ott, C. D. 2009, CQGra, 26, 063001
Özel, F., Psaltis, D., Narayan, R., & Villarreal, A. S. 2012, ApJ, 757, 55
Paczynski, B. 1991, AcA, 41, 257
Pan, Y., Buonanno, A., Taracchini, A., et al. 2014, PhRvD, 89, 084006
Pankow, C., Chatziioannou, K., Chase, E. A., et al. 2018, PhRvD, 98, 084016
Pannarale, F., & Ohme, F. 2014, ApJ, 791, L7
Piro, A. L., & Pfahl, E. 2007, ApJ, 658, 1173
Popham, R., Woosley, S. E., & Fryer, C. 1999, ApJ, 518, 356
Radice, D., Morozova, V., Burrows, A., Vartanyan, D., & Nagakura, H. 2019, ApJL, 876, L9
Salafia, O. S., Barbieri, C., Ascenzi, S., & Toffano, M. 2020, A&A, 636, A105
Sathyaprakash, B. S., & Dhurandhar, S. V. 1991, PhRvD, 44, 3819
Savchenko, V., Ferrigno, C., Kuulkers, E., et al. 2017, ApJL, 848, L15
Soni, S., Austin, C., Effler, A., et al. 2021, CQGra, 38, 025016
Stanek, K. Z., Matheson, T., Garnavich, P. M., et al. 2003, ApJL, 591, L17
Sun, L., Goetz, E., Kissel, J. S., et al. 2021, arXiv:2107.00129
Sutton, P. J., Jones, G., Chatterji, S., et al. 2010, NJPh, 12, 053034
Tan, W.-W., & Yu, Y.-W. 2020, ApJ, 902, 83
Taracchini, A., Buonanno, A., Pan, Y., et al. 2014, PhRvD, 89, 061502
Thorne, K. S. 1974, ApJ, 191, 507
Tohuvavohu, A., Kennea, J. A., DeLaunay, J., et al. 2020, ApJ, 900, 35
Troja, E., Piro, L., Ryan, G., et al. 2018, MNRAS, 478, L18
Troja, E., Piro, L., van Eerten, H., et al. 2017, Natur, 551, 71
Troja, E., van Eerten, H., Ryan, G., et al. 2019, MNRAS, 489, 1919
Tsang, D. 2013, ApJ, 777, 103
Tsang, D., Read, J. S., Hinderer, T., Piro, A. L., & Bondarescu, R. 2012, PhRvL, 108, 011102
van Putten, M. H., Levinson, A., Lee, H. K., et al. 2004, PhRvD, 69, 044007
van Putten, M. H. P. M. 2001, PhRvL, 87, 091101
van Putten, M. H. P. M., Lee, G. M., Della Valle, M., Amati, L., & Levinson, A. 2014, MNRAS, 444, L58
Vedrenne, G., & Atteia, J.-L. 2009, Gamma-Ray Bursts: The Brightest Explosions in the Universe (Heidelberg: Springer)
Vielfaure, J. B., Arabsalmani, M., Heintz, K. E., et al. 2019, GCN Circ., 26553, 1
Vielfaure, J. B., Xu, D., Palmerio, J., et al. 2020, GCN Circ., 26998, 1
Wanderman, D., & Piran, T. 2015, MNRAS, 448, 3026
Wang, X.-Y., & Mészáros, P. 2007, ApJ, 670, 1247
Was, M., Sutton, P. J., Jones, G., & Leonor, I. 2012, PhRvD, 86, 022003
Williamson, A. R., Biwer, C., Fairhurst, S., et al. 2014, PhRvD, 90, 122004
Woosley, S. E. 1993, ApJ, 405, 273
Zhang, B., & Mészáros, P. 2001, ApJL, 552, L35
Zhang, W., Woosley, S. E., & MacFadyen, A. I. 2003, ApJ, 586, 356